TABLE 1. Patient Characteristics

	Non-CAD (n=24)	SAP (n=45)	UAP (n=38)	P
Age, mean (range), y	62 (43–78)	65 (46–85)	66 (53–78)	0.36
Male sex, %	63	67	66	0.94
Degree of coronary stenosis, %		88.6 (74.8–94.3)	91.2 (74.6–95.0)	0.63
Ejection fraction, %	63 (51–77)	55 (40–69)	60 (41–70)	0.52
Hypertension, n (%)	12 (50)	32 (71)	20 (53)	0.13
Diabetes, n (%)	10 (42)	22 (49)	19 (50)	0.80
Hyperlipidemia, n (%)	9 (38)	21 (47)	20 (53)	0.62
Smoking, n (%)	10 (42)	19 (42)	17 (45)	0.96
Obesity, n (%)	9 (38)	20 (44)	15 (40)	0.83

Degree of coronary stenosis and ejection fraction are given as medians and interquartile ranges. Numbers of diseased vessels are given as mean and SEM.

ity.[16] BDNF induces oxidative stress via the activation of this oxidase system in cortical cells.[17] The localization of NTs in the cardiovascular system and their potent biological activities suggest a possible role for these neurotrophic molecules in the pathogenesis of cardiovascular disease, including acute coronary syndrome. To clarify the significance of NTs in the pathogenesis of CAD, we examined NT plasma levels in the coronary circulation of patients with angina pectoris and non-CAD and their regional expression in coronary arteries obtained from autopsied cases and coronary specimens obtained during directional coronary atherectomy (DCA). Furthermore, we examined the pro-oxidative effects of NTs on cultured vascular cells.

Methods

Patient Groups

Patients who underwent diagnostic coronary angiography and patients with angina in whom significant stenosis of the left coronary arteries was documented were enrolled. Subjects were divided into unstable angina (UAP), stable effort angina (SAP), and non-CAD groups. Table 1 shows the clinical characteristics of the 3 groups. The UAP group consisted of 38 patients who had anginal episodes at rest or angina during a mild degree of effort within 48 hours of the study without a significant increase in creatine phosphokinase levels. Patients were classified IB (n=14), IIB (n=12), and IIIB (n=12) according to Braunwald's criteria. The SAP group consisted of 45 patients with typical effort angina or positive treadmill exercise testing but no episodes of angina at rest. All patients with angina had >75% stenotic lesions in the left coronary artery determined by myocardial perfusion scintigraphy to be the culprit lesion. The non-CAD group consisted of 24 patients with chest pain syndrome (n=22) or mitral valve prolapse (n=2). They had no significant coronary artery stenosis >25% luminal diameter. No patients had acute infection, acute inflammation, or psychological disorders. No patients had taken antidepressant drugs, major tranquilizers, steroids, or nonsteroidal antiinflammatory drugs except for aspirin. Written informed consent was obtained from all patients before enrollment in the study.

Human Blood Samples

Before the injection of a contrast medium, blood samples were collected from the coronary sinus (Cs), aortic root (Ao), and femoral vein. At the time of blood sampling, the first 3 mL of blood was discarded, and additional blood was drawn into a tube containing EDTA (pH 7.5) for NT assay. The blood samples were immediately centrifuged at 3000 rpm for 10 minutes at 4°C, and the plasma was stored at −80°C until assayed.

Measurement of Plasma NT Levels

NTs were measured by sandwich ELISAs according to the manufacturer's instructions for BDNF and NT-3 (Promega). Assays were performed on polystyrene 96-well plates. The NT concentration was quantified against a standard curve calibrated with known amounts of protein. The detection limits were 4 pg/mL for BDNF and 8 pg/mL for NT-3. The BDNF or NT-3 ELISA systems have very low cross-reactivity with other related neurotrophic factors: 3% or 0.11% cross-reactivity, respectively. Each value is a mean of duplicated measurement.

Human Tissue and Immunohistochemistry

Human coronary arteries were collected from 11 autopsy cases within 6 hours after death. Table 2 shows the characteristics of the autopsy cases. Coronary arteries were removed from the heart and cut into 3-mm lengths. Before the immunohistochemical analysis, all autopsy sections were examined by hematoxylin and eosin staining and classified into nonatherosclerotic coronary arteries (n=7) and atherosclerotic arteries (n=13). Coronary specimens were obtained from patients with SAP (n=29) or UAP (n=21) during DCA.

Tissue distribution of BDNF was detected through the use of immunohistochemical methods according to the manufacturer's instructions for anti-human BDNF antibody (Chemicon International or Santa Cruz Biotechnology Inc). BDNF antibody has <0.1% cross-reactivity with recombinant human NT-3 or NT-4/5. Human tissues were fixed in Zamboni's fixative (4% formaldehyde, 15% picric acid in 0.1 mol/L phosphate buffer) for 2 hours and in 30% sucrose in PBS overnight at 4°C. Cryostat sections (20 μm) were blocked with 20% normal horse serum in PBS for 1 hour, followed by incubation with primary antibody diluted 1:500 in 2× PBS and

TABLE 2. Characteristics of Autopsy Cases

Sex	Age, y	Cause of Death	Associated Cardiovascular Disease(s)
Male	82	Hepatoma	Stable angina
Male	78	Pancreatic cancer	Hypertension
Male	73	Cardiac rupture	Acute myocardial infarction
Male	70	Congestive heart failure	Old myocardial infarction
Female	66	Hepatoma	Hypertension
Male	65	Lung cancer	None
Female	64	Lymphoma	Hypertension
Male	63	Colon cancer	None
Male	51	Congestive heart failure	Dilated cardiomyopathy
Male	41	Sudden death	Ventricular tachycardia
Male	35	Gastric cancer	None

0.3% Triton X-100 containing 0.02% sodium azide. After a 24-hour incubation at room temperature, the samples were washed and incubated with biotinylated goat anti-rabbit immunoglobulin (DAKO). For color development, we used an LSAB kit (DAKO). For a negative control, the primary antibody was replaced with rabbit serum.

Double-Labeling Immunofluorescence

The antibodies used in double staining were mouse monoclonal anti-human CD68 antibody (DAKO) for macrophages and mouse monoclonal anti-human smooth muscle α-actin antibody (DAKO) for smooth muscle cells. Texas red–conjugated anti-mouse immunoglobulin and FITC-conjugated anti-rabbit immunoglobulin were applied as secondary antibodies. The samples were examined by a laser scanning confocal imaging system (MRC-1024, Bio-Rad Laboratories).

Semiquantitative Analysis of BDNF in Immunohistochemistry

According to a previous study, the expression of BDNF in each DCA specimens was graded as follows: grade 0=negative stain, grade 1=variable or weak stain, and grade 2=moderately or strongly positive stain.[18] The sections were blindly graded by 3 independent senior pathologists.

Measurement of NAD(P)H Oxidase Activity in Human Coronary Artery Smooth Muscle Cells

Human coronary artery smooth muscle cells (CASMCs; Clonetics) were cultured with medium (Clonetics) supplemented with 10% FBS and the manufacturer's reagents (Clonetics).

The enzymatic activity of NAD(P)H oxidase in human CASMC homogenates was assessed by lucigenin-enhanced chemiluminescence (L-CL). Human CASMCs were preincubated with or without 100 ng/mL BDNF for 1 hour; suspended in homogenate buffer containing 50 mmol/L Tris/HCL (pH 7.4), 1.0 mmol/L EDTA, 500 mmol/L phenylmethylsulfonyl fluoride, 2.0 mmol/L leupeptin, and 2.0 mmol/L pepstatin A; and then homogenized with an ultrasonicator (4×15 seconds) on ice. In the time-course study, the cells were incubated for each period with 100 ng/mL BDNF; in the dose-response study, they were stimulated with the indicated concentration of BDNF for 1 hour. The assay solution contained 50 mmol/L HEPES (pH 7.4), 1.0 mmol/L EDTA, 6.5 mmol/L $MgCl_2$, 5.0 μmol/L lucigenin as an electron acceptor, and either 1 mmol/L NADH or 1 mmol/L NADPH as a substrate. After preincubation at 37°C for 10 minutes, the reaction was started by adding 100 μL cell homogenate. The final volume of the reaction solution was 1.0 mL. Photon emission was recorded continuously for 20 minutes. The chemiluminescent signals observed in the absence of homogenates were subtracted from the chemiluminescence signals of the samples. The chemiluminescence signal was corrected for the protein concentration of each cell homogenate and expressed as counts per minute per milligram protein for an average 20-minute period. In some experiments, the cell homogenates were preincubated with 10 μmol/L diphenylene iodonium (DPI), a selective NAD(P)H oxidase inhibitor, for 20 minutes before L-CL measurement.

Superoxide Production From Human CASMCs

Dihydroethidium oxidative fluorescence dye was used to evaluate in situ production of superoxide. Human CASMCs were preincubated with or without 100 ng/mL BDNF for 1 hour, treated with dihydroethidium (10 μmol/L), and then capped with coverslips. The slides were incubated in a light-protected humidified chamber at 37°C for 20 minutes. The dihydroethidium image was obtained by a laser scanning confocal imaging system (MRC-1024) equipped with a 585-nm long-pass filter.

TABLE 3. BDNF and NT-3 Concentration in Cs, Ao, and Peripheral Vein

	Non-CAD, pg/mL	SAP, pg/mL	UAP, pg/mL	*P*
BDNF				
Cs	1308 (822–1711)	1206 (683–1608)	1503 (1123–2350)	0.67
Ao	1347 (781–1743)	1229 (697–1705)	1249 (776–1754)	0.53
V	1297 (654–1856)	1267 (781–1706)	1304 (802–1689)	0.78
NT-3				
Cs	511 (460–555)	459 (380–546)	433 (308–807)	0.51
Ao	498 (345–587)	428 (360–530)	430 (332–753)	0.76
V	492 (387–606)	445 (365–530)	442 (321–799)	0.77

V indicates peripheral vein. All values are given as medians and interquartile ranges. Probability values are for the comparison among the 3 groups.

Statistical Analysis

Data are expressed as medians and interquartile ranges, medians and ranges, or means and SEM as appropriate. Statistical comparison for categorical variables such as risk factors and sex was performed by the χ^2 test. Age and left ventricle ejection fraction were compared between groups with 1-way ANOVA. Statistical comparison for coronary stenosis between the SAP and UAP groups and the NAD(P)H oxidase activity was performed by the nonparametric tests; the Mann-Whitney was used for comparison. Statistical comparison for NT plasma levels was performed by the nonparametric Kruskal-Wallis tests with multiple-comparison post-hoc procedures (Dunn's method). Statistical analysis was performed with StatView 5 software (SAS Institute, Inc). A value of $P<0.05$ was considered to indicate statistical significance.

Results

Patient Characteristics

Table 1 shows the clinical characteristics of the 3 groups. There were no statistical differences among the 3 groups in the following variables: age, sex, left ventricular ejection fraction, hypertension, diabetes mellitus, hyperlipidemia, smoking, or obesity. There were no significant differences between the UAP and SAP groups in the number of diseased vessels or the degree of angiographic stenosis. There was no difference in the standard medications between the UAP and SAP patients.

BDNF in Coronary Circulation Was Increased in Unstable Angina

There was no difference in plasma levels of BDNF and NT-3 among the 3 groups (Table 3). To examine coronary circulation–specific levels of NTs, the difference in NT levels between the Cs and Ao was calculated. The Cs-Ao difference in plasma BDNF in the UAP group was significantly greater than that in the SAP and non-CAD groups, whereas there was no Cs-Ao difference in NT-3 among the groups (Figure 1).

TABLE 4. Semiquantitative Analysis of BDNF in Coronary Specimens Obtained by DCA

	Expression Scores
SAP (n=29)	0.57 (0.33–1.33)
UAP (n=21)	1.74 (1.0–2.33)*

For expression scores, negative stain=0, weak stain=1, and moderate or strong stain=2. All values are given as medians and interquartile range.

*Significant differences between UAP and SAP, $P<0.01$.

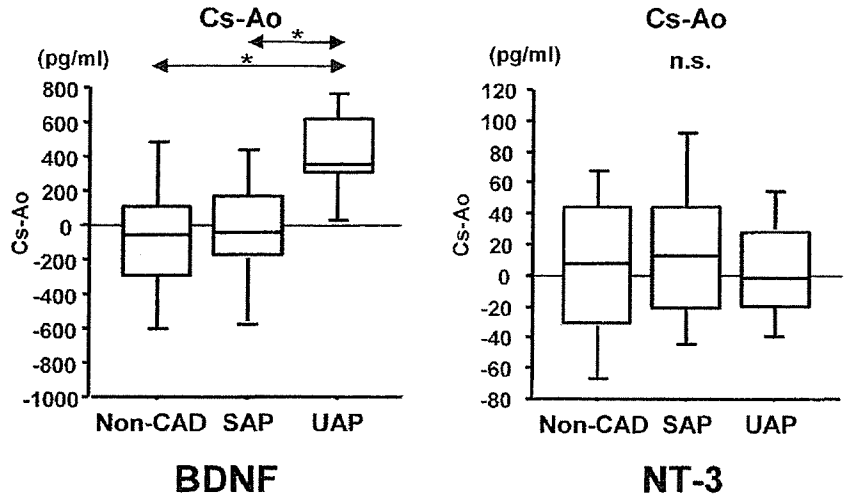

Figure 1. Cs-Ao differences in plasma NT levels across the coronary circulation. The Cs-Ao differences in plasma BDNF were significantly greater in the UAP group than in the SAP or non-CAD group, whereas the Cs-Ao differences in NT-3 were not significantly different among the 3 groups. Data are expressed as medians, with 25th and 75th percentiles (boxes) and 10th and 90th percentiles (I bars). *$P<0.01$ for the comparisons of the UAP, SAP, and non-CAD groups.

These findings indicate that the generation of BDNF in the coronary circulation was enhanced in patients with UAP.

BDNF Expression in Human Coronary Artery

The blood sampling results (Figure 1) led us to examine BDNF expression in the coronary arteries. Immunohistochemical analysis of coronary arteries obtained from autopsy cases was performed. BDNF was expressed in atherosclerotic coronary arteries in all specimens (Figure 2). BDNF was preferentially localized in the atheromatous intima and around the vasa vasorum in the adventitia (Figure 2D and 2E). In contrast, BDNF immunoreactivity was barely detected in nonatherosclerotic coronary arteries (Figure 2C).

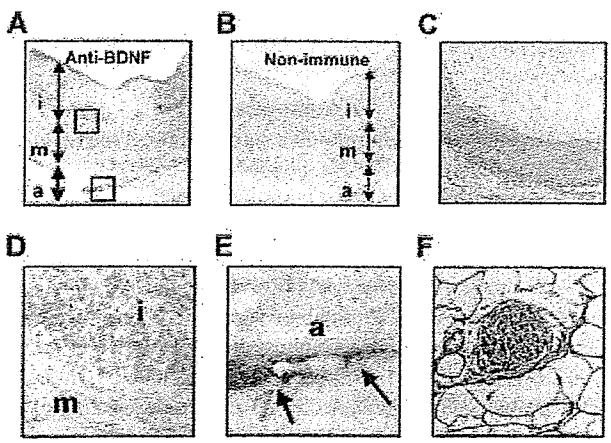

Figure 2. BDNF expression in human coronary arteries of autopsy cases. A, Low-power view of representative human atherosclerotic coronary arteries obtained from autopsied cases shows intense BDNF immunoreactivity in the atherosclerotic intima (i) and adventitia (a). B, There is no significant staining with nonimmune serum used as a control. C, Low-power view of representative nonatherosclerotic coronary arteries shows negligible immunoreactivity of BDNF. D, High-power view of the area indicated by the rectangle in A shows BDNF expression in smooth muscle cells of the intima. E, High-power view of the area indicated by the rectangle in B shows the expression of BDNF in fibroblasts around the vasa vasorum in the adventitia. F, Immunostaining of BDNF in peripheral nerves in pericardial tissues. m Indicates media.

Figure 2F shows BDNF expression in peripheral nerves. Double staining with cell-specific markers using serial sections revealed that some smooth muscle cells and macrophages expressed BDNF (Figure 3).

BDNF Expression in Coronary Specimens of Patients With Angina Pectoris

Investigation of coronary specimens from DCA of patients with SAP (n=29) and UAP (n=21) revealed enhanced BDNF expression in inflammatory cells, smooth muscle cells, and extracellular matrix (Figure 4). To investigate the

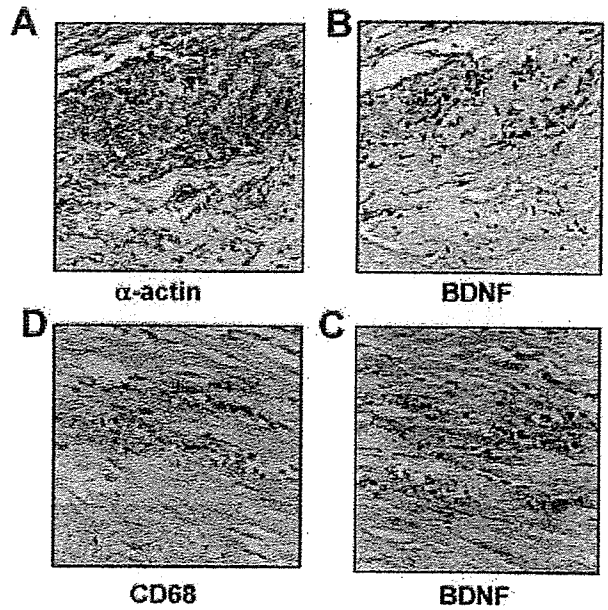

Figure 3. Association between BDNF and CD-68 or α-actin in atherosclerotic coronary arteries. A, B, Immunohistochemical staining of α-actin, a marker of smooth muscle cells (A), and BDNF (B) in serial sections of atherosclerotic coronary arteries of autopsy sample, showing that some smooth muscle cells expressed BDNF. C, D, Immunohistochemical staining of CD-68, a marker of macrophages (C), and BDNF (D) in serial sections of atherosclerotic coronary arteries of autopsy samples, showing that macrophages expressed BDNF.

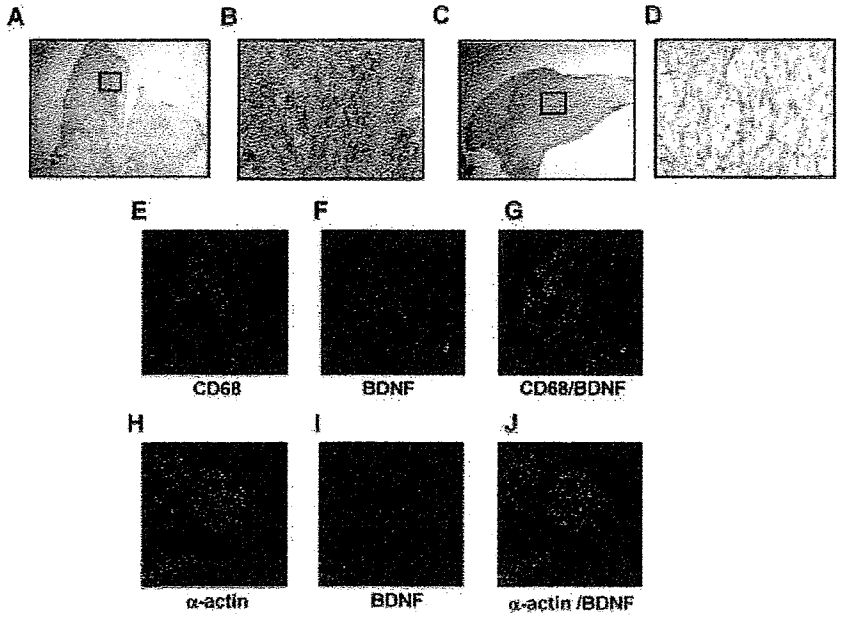

Figure 4. BDNF expression in DCA specimens. Low-power (A, C) and high-power (B, D) views of representative staining for BDNF of DCA specimens from angina patients. Immunohistochemical analysis revealed BDNF expression in inflammatory cells, smooth muscle cells, and extracellular matrix. E–J, Double immunofluorescence of BDNF with cell-specific markers. Anti-CD68 (E) and anti–α-actin (H) were used as markers of macrophage and smooth muscle cells, respectively. Red-labeled immunofluorescence indicates cell makers; green-labeled immunofluorescence indicates expression of BDNF (F, I). Colocalization of cell-specific makers and BDNF is shown by yellow-labeled immunofluorescence (G, J). Representative figure (n=5) is shown, and similar results were observed in all examinations.

cell types of BDNF-expressing cells, double immunofluorescence of BDNF and CD68 or α-actin, a specific marker of macrophages and smooth muscle cells, respectively, was carried out. As shown in Figure 4E through 4J, smooth muscle cells and macrophages expressed BDNF in coronary specimens of patients with angina pectoris.

Semiquantitative analysis demonstrated that BDNF expression in coronary arteries of UAP patients was more intense compared with SAP (Table 4). Representative cases of UAP and SAP are shown in Figure 5.

BDNF Enhanced NAD(P)H Oxidase Activity and Reactive Oxygen Species in Human CASMCs

The effects of BDNF on NAD(P)H oxidase activity were examined in human CASMCs. Stimulation with 100 ng/mL BDNF increased NADH- and NADPH-dependent oxidase activity ≈2.7- and 2.3-fold compared with that in control (nontreated) cells, respectively (Figure 6A). This oxidative activity was reduced by 10 μmol/L DPI, a selective inhibitor of NAD(P)H oxidase. In the presence of DPI, NADH- and NADPH-dependent oxidase activity in CASMCs was reduced by 74% and 45%, respectively. The effects of BDNF on NAD(P)H oxidase activity were dose and time dependent (Figure 6B). Furthermore, in experiments with dihydroethidium, an intracellular fluorescence probe, BDNF stimulation increased the generation of reactive oxygen species (Figure 6C).

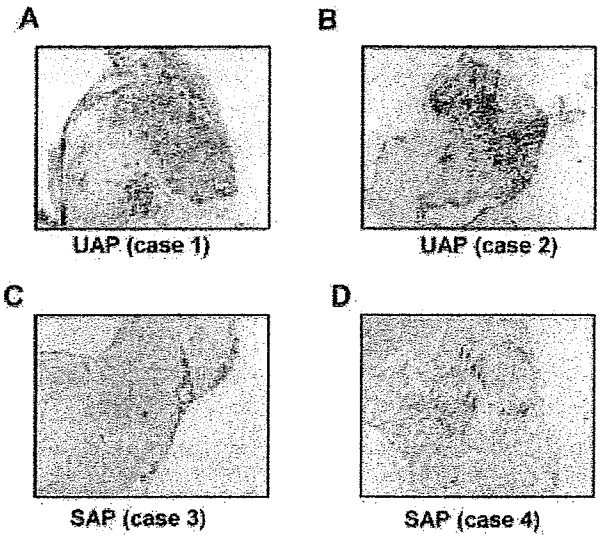

Figure 5. BDNF expression in coronary specimens of patients with angina pectoris. A B, Representative cases of UAP; C, D, representative cases of SAP. Semiquantitative analysis is shown in Table 4.

Discussion

The present study demonstrated a significantly greater Cs-Ao difference in plasma BDNF, but not NT-3, in the UAP group than in the SAP and non-CAD groups. Immunohistochemical analysis revealed that BDNF was expressed in atheromatous intima and adventitia in human coronary arteries. Intense BDNF immunoreactivity was observed in macrophages and smooth muscle cells in atherosclerotic coronary arteries. Semiquantitative analysis demonstrated that BDNF expression in UAP patients was more intense compared with SAP. Furthermore, BDNF enhanced NAD(P)H oxidase activity and superoxide production in cultured CASMCs, and its selective inhibitor suppressed the effect of BDNF. Thus, BDNF in the coronary vasculature might enhance oxidative stress via the activation of NAD(P)H oxidase.

BDNF has protective effects against injury or ischemia in both the central and peripheral nervous systems.[4–6] For example, Schabitz et al[19] demonstrated that intravenous BDNF injection reduces infarct size in rat model. On the other hand, several lines of evidence suggest that NTs potentiate neuronal death under some conditions such as serum or oxygen-glucose deprivation.[20,21] Kim et al[17] demonstrated that BDNF acts as a pronecrotic factor through activation of NAD(P)H oxidase in cortical cells, and other

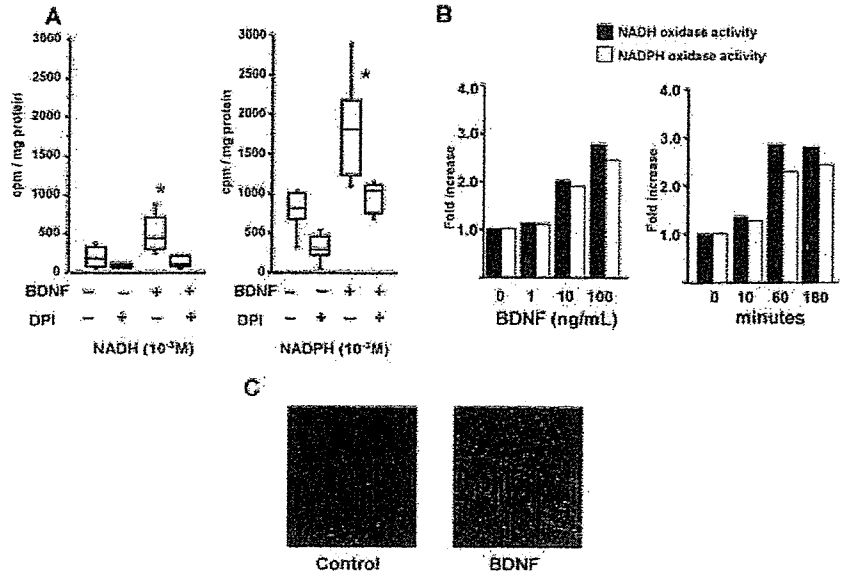

Figure 6. A, Effect of BDNF on NAD(P)H oxidase in cultured human CASMCs. Enzymatic activity of NAD(P)H oxidase in human CASMC homogenates was assessed by L-CL. NADH- (left) and NADPH- (right) dependent oxidase activity was enhanced by treatment with BDNF (100 ng/mL) for 1 hour. Treatment with DPI reduced the activity of NAD(P)H oxidase. The chemiluminescent signals are expressed as counts per minute per milligrams of protein. Data are expressed as medians, with 25th and 75th percentiles (boxes) and 10th and 90th percentiles (I bars). B, Dose response and time dependency of BDNF on NAD(P)H oxidase activity. In the dose-response study, CASMCs were stimulated with the indicated concentration of BDNF for 1 hour (left). In the time-course study, the cells were incubated for each period with 100 ng/mL BDNF (right). Graphs are representatives of 4 independent experiments. *$P<0.05$ for the chemiluminescent signals of CASMCs with and without BDNF preincubation. C, Effect of BDNF on reactive oxygen species generation in cultured human CASMCs. Generation of reactive oxygen species was assessed with the dihydroethidium method. Treatment with BDNF (100 ng/mL) increased superoxide generation vs control. Results are representative of 5 independent experiments.

studies indicated that NTs induce cell death in cerebral ischemia.[22] Thus, the intracellular signaling pathway mediated by NTs can act not only for survival but also as a proapoptotic or pronecrotic pathway in neuronal cells. Whether coronary BDNF induces cell necrosis or apoptosis of vascular cells warrants further investigation. BDNF enhanced the activity of NAD(P)H oxidase and the generation of superoxide in cultured smooth muscle cells. Because oxygen radicals activate matrix metalloproteinases,[23] the oxidative stress by BDNF might induce the instability of atherosclerotic plaques. On the other hand, BDNF has important roles in survival or as a development factor even in nonneuronal tissues such as endothelial cells.[24] BDNF in vasculature may work as a protective factor for endothelial cells in a counterregulatory mechanism. Further investigation is needed to clarify the precise mechanisms of BDNF in the pathogenesis of UAP.

In the present investigation, increased Cs-Ao differences in BDNF were observed in the UAP patents, although there was no significant difference in the numbers of diseased vessels or the degree of coronary stenosis between the SAP and UAP groups. These findings indicate that BDNF in the coronary circulation seems to influence the disease state of angina pectoris rather than the degree of coronary atherosclerosis and plaque formation. Acute coronary syndrome usually occurs at sites with <70% stenosis, as determined by angiographic studies performed in patients before the onset of coronary events. Therefore, BDNF might be involved in the vulnerability of atherosclerotic plaques. There are several possible origins of BDNF in the coronary circulation, including vascular smooth muscle cells, accumulating inflammatory cells, adventitial fibroblasts, cardiac myocytes, and neural cells. Recently, it has been reported that platelets release BDNF; therefore, activated platelets are a potential origin of BDNF.[25] However, the intense immunoreactivity in patients with UAP suggests that BDNF in the coronary circulation likely comes from atherosclerotic plaques. Plaque rupture and erosion are key events in the pathogenesis of acute coronary syndrome, including unstable angina; therefore, it is possible that disrupted atherosclerotic plaques release BDNF. Some other factors may be involved in the increased Cs-Ao differences in BDNF. Thus, further investigations are necessary to establish the causal relationship between BDNF and plaque rupture.

Psychological stress produces significant increases in heart rate and blood pressure, which might lead to an increased myocardial oxygen demand. Kario et al[26] demonstrated that earthquake-induced stress increased not only blood pressure and blood viscosity determinants but also fibrin turnover with endothelial cell stimulation in a group of hypertensive elderly subjects, suggesting that acute stress might trigger cardiovascular events. On the other hand, psychological stress increases the secretion of NTs from central and peripheral nerves.[27–29] Neuropsychological studies demonstrate that psychological stress such as immobilization stress increases BDNF mRNA expression in the hypothalamus of experimental models.[29] There is no direct evidence that BDNF in the coronary vasculature is regulated by psychological stress in

humans; however, psychological stress might increase the production of BDNF in coronary beds, which in turn augments regional oxidative stress via NAD(P)H oxidase. Further investigation is needed to clarify the regulation of coronary BDNF and the direct effect of psychological stress on NT levels in the coronary vasculature.

Plasma BDNF levels are decreased in patients with psychological disorders such as depression, and the level recovers with antidepressant drug treatment.[27,30] In our study, we did not enroll patients with mental disorders, and no patients had taken antidepressant drugs or tranquilizers. Although the psychological states of the patients were not examined, we do not consider that the Cs-Ao differences in BDNF were influenced by these factors.

In conclusion, plasma BDNF, but not NT-3, was increased in the coronary circulation in patients with UAP, and BDNF expression was enhanced in coronary arteries of UAP patients. BDNF increased NAD(P)H oxidase activity and superoxide production in human CASMC culture. Our observations suggest that the enhanced oxidative stress induced by BDNF has an important role in plaque instability.

References

1. Ogawa K, Tsuji I, Shiono K, Hisamichi S. Increased acute myocardial infarction mortality following the 1995 great Hanshin-Awaji earthquake in Japan. *Int J Epidemiol.* 2000;29:449–455.
2. Rozanski A, Blumenthal JA, Kaplan J. Impact of psychological factors on the pathogenesis of cardiovascular disease and implications for therapy. *Circulation.* 1999;99:2192–2217.
3. Barde YA, Edgar D, Thoenen H. Purification of a new neurotrophic factor from mammalian brain. *EMBO J.* 1982;1:549–553.
4. Hohn A, Leibrock J, Bailey K, Barde YA. Identification and characterization of a novel member of the nerve growth factor/brain-derived neurotrophic factor family. *Nature.* 1990;344:339–341.
5. Lewin GR, Barde YA. Physiology of the neurotrophins. *Annu Rev Neurosci.* 1996;19:289–317.
6. DiStefano PS, Friedman B, Radziejewski C, Alexander C, Boland P, Schick CM, Lindsay RM, Wiegand SJ. The neurotrophins BDNF, NT-3, and NGF display distinct patterns of retrograde axonal transport in peripheral and central neurons. *Neuron.* 1992;8:983–993.
7. Lessmann V, Gottmann K, Malcangio M. Neurotrophin secretion: current facts and future prospects. *Prog Neurobiol.* 2003;69:341–374.
8. Patapoutian A, Reichardt LF. Trk receptors: mediators of neurotrophin action. *Curr Opin Neurobiol.* 2001;11:272–280.
9. Roux PP, Barker PA. Neurotrophin signaling through the p75 neurotrophin receptor. *Prog Neurobiol.* 2002;67:203–233.
10. Clegg DO, Large TH, Bodary SC, Reichardt LF. Regulation of nerve growth factor mRNA levels in developing rat heart ventricle is not altered by sympathectomy *Dev Biol.* 1989;134:30–37.
11. Yamamoto M, Sobue G, Yamamoto K, Terao S, Mitsuma T. Expression of mRNAs for neurotrophic factors (NGF, BDNF, NT-3, and GDNF) and their receptors (p75NGFR, trkA, trkB, and trkC) in the adult human peripheral nervous system and nonneural tissues. *Neurochem Res.* 1996; 21:929–938.
12. Donovan MJ, Miranda RC, Kraemer R, McCaffrey TA, Tessarollo L, Mahadeo D, Sharif S, Kaplan DR, Tsoulfas P, Parada L, et al. Neurotrophin and neurotrophin receptors in vascular smooth muscle cells: regulation of expression in response to injury. *Am J Pathol.* 1995;147: 309–324.
13. Barouch R, Appel E, Kazimirsky G, Brodie C. Macrophages express neurotrophins and neurotrophin receptors: regulation of nitric oxide production by NT-3. *J Neuroimmunol.* 2001;112:72–77.
14. Kerschensteiner M, Gallmeier E, Behrens L, Leal VV, Misgeld T, Klinkert WE, Kolbeck R, Hoppe E, Oropeza-Wekerle RL, Bartke I, Stadelmann C, Lassmann H, Wekerle H, Hohlfeld R. Activated human T cells, B cells, and monocytes produce brain-derived neurotrophic factor in vitro and in inflammatory brain lesions: a neuroprotective role of inflammation? *J Exp Med.* 1999;189:865–870.
15. Nakahashi T, Fujimura H, Altar CA, Li J, Kambayashi J, Tandon NN, Sun B. Vascular endothelial cells synthesize and secrete brain-derived neurotrophic factor. *FEBS Lett.* 2000;470:113–117.
16. Azumi H, Inoue N, Ohashi Y, Terashima M, Mori T, Fujita H, Awano K, Kobayashi K, Maeda K, Hata K, Shinke T, Kobayashi S, Hirata K, Kawashima S, Itabe H, Hayashi Y, Imajoh-Ohmi S, Itoh H, Yokoyama M. Superoxide generation in directional coronary atherectomy specimens of patients with angina pectoris: important role of NAD(P)H oxidase. *Arterioscler Thromb Vasc Biol.* 2003;22:1838–1844.
17. Kim SH, Won SJ, Sohn S, Kwon HJ, Lee JY, Park JH, Gwag BJ. Brain-derived neurotrophic factor can act as a pronecrotic factor through transcriptional and translational activation of NADPH oxidase. *J Cell Biol.* 2002;159:821–831.
18. Azumi H, Inoue N, Takeshita S, Rikitake Y, Kawashima S, Hayashi Y, Itoh H, Yokoyama M. Expression of NADH/NADPH oxidase p22phox in human coronary arteries. *Circulation.* 1999;100:1494–1498.
19. Schabitz WR, Schwab S, Spranger M, Hacke W. Intraventricular brain-derived neurotrophic factor reduces infarct size after focal cerebral ischemia in rats. *J Cereb Blood Flow Metab.* 1997;17:500–506.
20. Huang BR, Gu JJ, Ming H, Lai DB, Zhou XF. Differential actions of neurotrophins on apoptosis mediated by the low affinity neurotrophin receptor p75NTR in immortalised neuronal cell lines. *Neurochem Int.* 2000;36:55–65.
21. Ishikawa Y, Ikeuchi T, Hatanaka H. Brain-derived neurotrophic factor accelerates nitric oxide donor-induced apoptosis of cultured cortical neurons. *J Neurochem.* 2000;75:494–502.
22. Bates B, Hirt L, Thomas SS, Akbarian S, Le D, Amin-Hanjani S, Whalen M, Jaenisch R, Moskowitz MA. Neurotrophin-3 promotes cell death induced in cerebral ischemia, oxygen-glucose deprivation, and oxidative stress: possible involvement of oxygen free radicals. *Neurobiol Dis.* 2002;9:24–37.
23. Inoue N, Takeshita S, Gao D, Ishida T, Kawashima S, Akita H, Tawa R, Sakurai H, Yokoyama M. Lysophosphatidylcholine increases the secretion of matrix metalloproteinase 2 through the activation of NADH/NADPH oxidase in cultured aortic endothelial cells. *Atherosclerosis.* 2001;155:45–52.
24. Donovan MJ, Lin MI, Wiegn P, Ringstedt T, Kraemer R, Hahn R, Wang S, Ibanez CF, Rafii S, Hempstead BL. Brain derived neurotrophic factor is an endothelial cell survival factor required for intramyocardial vessel stabilization. *Development.* 2000;127:4531–4540.
25. Fujimura H, Altar CA, Chen R, Nakamura T, Nakahashi T, Kambayashi J, Sun B, Tandon NN. Brain-derived neurotrophic factor is stored in human platelets and released by agonist stimulation. *Thromb Haemost.* 2002;87:728–734.
26. Kario K, Matsuo T, Kayaba K, Soukejima S, Kagamimori S, Shimada K. Earthquake-induced cardiovascular disease and related risk factors in focusing on the great Hanshin-Awaji earthquake. *J Epidemiol.* 1998;8: 131–139.
27. Smith MA, Makino S, Altemus M, Michelson D, Hong SK, Kvetnansky R, Post RM. Stress and antidepressants differentially regulate neurotrophin 3 mRNA expression in the locus coeruleus. *Proc Natl Acad Sci USA.* 1995;92:8788–8792.
28. Russo-Neustadt A. Brain-derived neurotrophic factor, behavior, and new directions for the treatment of mental disorders. *Semin Clin Neuropsychiatry.* 2003;8:109–118.
29. Rage F, Givalois L, Marmigere F, Tapia-Arancibia L, Arancibia S. Immobilization stress rapidly modulates BDNF mRNA expression in the hypothalamus of adult male rats. *Neuroscience.* 2002;112:309–318.
30. Shimizu E, Hashimoto K, Okamura N, Koike K, Komatsu N, Kumakiri C, Nakazato M, Watanabe H, Shinoda N, Okada S, Iyo M. Alterations of serum levels of BDNF in depressed patients with or without antidepressants. *Bio Psychiatry.* 2003;54:70–75.

ELSEVIER

Cardiovascular Research 68 (2005) 249 – 258

Cardiovascular Research

www.elsevier.com/locate/cardiores

Xenogenic smooth muscle cell immunization reduces neointimal formation in balloon-injured rabbit carotid arteries

Masakazu Shinohara, Seinosuke Kawashima *, Tomoya Yamashita, Tomofumi Takaya, Ryuji Toh, Tatsuro Ishida, Tomomi Ueyama, Nobutaka Inoue, Ken-ichi Hirata, Mitsuhiro Yokoyama

Division of Cardiovascular and Respiratory Medicine, Department of Internal Medicine, Kobe University Graduate School of Medicine, 7-5-1 Kusunoki-cho, Chuo-ku, Kobe 650-0017, Japan

Received 6 October 2004; received in revised form 20 June 2005; accepted 22 June 2005
Available online 21 July 2005
Time for primary review 20 days

Abstract

Objective: Intimal hyperplasia plays an important role in a variety of types of vascular remodeling, particularly luminal narrowing after vascular injury. The vascular smooth muscle cells (VSMCs) in the neointimal area are a synthetic phenotype and have different epitopes from VSMCs in the normal media. The synthetic VSMCs in the neointima contain various possible antigens that can be targeted by the immune system. In this study, we tried to develop a new immunotherapy, which targets the synthetic VSMCs, for prevention of neointimal formation after angioplasty.

Method and results: Rabbits were repeatedly immunized with fixed xenogenic rat cultured VSMCs suspended in adjuvant as immunogens or injected with adjuvant and phosphate-buffered saline (PBS) or rat hepatocytes as controls every 2 weeks for 3 times. One week after the last immunization/injection, balloon injury of the left common carotid artery was performed. Four weeks after the injury, rabbits were euthanized and the neointimal lesion formation was assessed. The mean neointimal area of the PBS-injected, non-immunized group and the rat hepatocyte-immunized, control group was not statistically different (0.339 ± 0.036 and 0.350 ± 0.041 mm^2, P=NS). However, immunization with rat VSMCs significantly reduced the intimal lesion area (0.219 ± 0.0286 mm^2; $P<0.05$ vs. PBS-injected, non-immunized group and rat hepatocyte-immunized group.) PCNA-immunopositive proliferating VSMCs in the neointima were suppressed by the rat VSMC immunization ($1.34 \pm 0.49\%$ vs. $5.78 \pm 0.47\%$; $P<0.05$ vs. PBS-injected, non-immunized group). Rat VSMC immunization induced antibodies which had strong cross-reactivity against rabbit synthetic VSMCs. In experiments in vitro, proliferation and migration of rabbit VSMCs that were stimulated by serum, angiotensin (AT) II, platelet-derived growth factor (PDGF)-BB, fibroblast growth factor (FGF), and the phorbol ester PMA were significantly suppressed by treatment with immunoglobulin extracted from the VSMC-immunized rabbit plasma, implying that the immunoglobulin had some global effects on VSMCs. The rat VSMC-immunized rabbit immunoglobulin bound the rabbit AT1a receptor protein, which was expressed in COS7 cells by transfection of rabbit AT1a receptor pcDNA3. This binding to AT1a receptor may be one of mechanisms of the effects of VSMC-immunized immunoglobulin.

Conclusion: Xenogenic, synthetic rat VSMC immunization in rabbits induced auto-antibodies against synthetic rabbit VSMCs in a cross-reaction. The induced auto-antibodies against synthetic VSMCs may provide a possibility of new immunotherapy for vascular remodeling that forms neointimal lesions.

Keywords: Neointimal formation; Vascular remodeling; Vascular smooth muscle; Antibody; Immunotherpy

* Corresponding author. Tel.: +81 78 382 5846; fax: +81 78 382 5859.
E-mail address: kawashim@med.kobe-u.ac.jp (S. Kawashima).

0008-6363/$ - see front matter © 2005 European Society of Cardiology. Published by Elsevier B.V. All rights reserved.
doi:10.1016/j.cardiores.2005.06.016

This article is referred to in the Editorial by Thaunat et al. (pages 183–185) in this issue.

1. Introduction

Intimal hyperplasia plays an important role in a variety of types of vascular remodeling, particularly luminal narrowing after vascular injury such as that seen in restenosis following percutaneous coronary intervention. Proliferation and migration of vascular smooth muscle cells (VSMCs) from the media play a central role in neointimal formation, and various strategies have been developed to inhibit it, including inhibition of cell cycle of VSMCs, induction of apoptosis of VSMCs, and inhibition of intracellular signal transduction in VSMCs [1–4].

Recently immunological modulation has attracted attention as a possible therapeutic strategy of atherosclerosis [5–22]. Although only limited information is available, several studies have shown the possibility of immunotherapy against neointimal lesion formation after balloon injury. It seems that adequate induction of B-lymphocyte-related immunity has potential beneficial effects on neointimal formation. Nilsson et al. showed that immunization with homologous oxidized low density lipoprotein reduced neointimal formation after balloon injury in hypercholesterolemic rabbits [23]. In balloon-injured rat carotid arteries, it was demonstrated that treatment with an anti-P selectin monoclonal antibody reduced inflammation, in neointimal formation, and vascular remodeling [24]. However, until now, only few epitopes have been reported as appropriate targets of immunotherapy against neointimal formation.

It is possible that synthetic VSMCs in the neointima contain various possible antigens that can be targeted by the immune system. Since VSMCs play a central role in neointimal formation, we hypothesized that immune modulation targeting the synthetic VSMCs-associated antigens may inhibit neointimal formation after balloon injury. To prove this hypothesis, rabbits were immunized with the synthetic xenogenic rat VSMCs and then balloon-injured to induce neointimal formation.

2. Methods

2.1. Materials and animals

All drugs and culture media used in this study were purchased from Sigma Chemical Co. (MO) and WAKO (Japan). Male Japanese White Rabbits were purchased from a breeder (SLC, Hamamatsu, Japan) and kept under conventional conditions in our animal facility. Rabbits were fed normal chow (Oriental Yeast, Japan) and water ad libitum and maintained on a 12 h light/dark cycle. All animal experiments were conducted according to the "Guidelines for Animal Experiments at Kobe University Graduate School of Medicine", which complies NIH Guidelines.

2.2. Preparation for rat vascular smooth muscle cells and rat hepatocytes as immunogens

Rat VSMCs were prepared from thoracic aortas of male Sprague–Dawley rats by the collagenase digestion method and cultured as described [25]. For all experiments, rat aortic VSMCs from passage 5 to 8 were used. Rat hepatocytes (RLC-18, Cell No. RCB1484) were purchased from Rikken Cell Bank (Japan).

Rat VSMCs and rat hepatocytes were cultured in DMEM with 10% fetal bovine serum (FBS), and approximately 1×10^8 cells were collected and washed three times with phosphate buffered saline (PBS). The cells were fixed with 10% neutralized formaldehyde (WAKO, Japan) for 24 h at 4 °C. After being washed three times and incubated at 37 °C for 2 h to remove residual formaldehyde, the cells were washed again and re-suspended in PBS for use as immunogens.

2.3. Experimental protocol

Male Japanese White Rabbits (body weights were 2.0 kg) were divided into three groups. Injection of either rat VSMCs as immunogens (1×10^8 cells per rabbit), vehicle PBS for control non-immunized group or rat hepatocytes (1×10^8 cells per rabbit) for control immunized group was started. Those injections were subcutaneously performed in the rabbits' back with an equal volume of adjuvant every two weeks for three times. We used the Freund complete adjuvant for the first immunization, and the Freund incomplete adjuvant for the second and the third immunization.

One week after the last injection, rabbits were anesthetized with sodium pentothal. Blood sample was collected from the ear vein. Plasma immunoglobulin (IgG) levels were assessed using a commercially available kit (Bethyl Laboratories Inc. TX). A 2F Fogarty embolectomy catheter (Baxter, USA) was introduced through an aseptic neck incision produced in the facial branch of the external left carotid artery and positioned approximately at the origin of the common carotid artery. An acute balloon injury was performed by inflating the balloon with 0.1 mL saline solution and then gently pulling it back along the entire length of the common carotid artery with constant rotation as described before [26]. The catheter was then removed, the artery branch was ligated, and the surgical wound was closed. Two and four weeks after balloon injury, rabbits were euthanized, and the neointimal lesion formation was assessed.

2.4. Histological and immunohistochemical analysis of neointimal lesions

Serial equally spaced cross sections (5 μm thick) were obtained throughout the entire length of the carotid artery

for histological analysis (average of six sections per animal). All samples were routinely stained with hematoxyline and eosin or subjected to immunostaining with the anti-proliferating cell nuclear antigen (PCNA). For immunohistochemistry, slides were preincubated with 1% bovine serum to decrease nonspecific binding. Sections were incubated overnight at 4 °C with the mouse anti-PCNA antibody (DAKO, Denmark).

2.5. Quantification of neointimal lesions in sections of carotid arteries

Six equally spaced cross sections of the entire length of carotid arteries were used in all rabbits to quantify neointimal lesions. Using NIH imaging software, total cross-sectional neointimal area was measured between the endothelial cell monolayer and the internal elastic lamina. Total cross-sectional medial area was measured between the external and internal elastic lamina.

2.6. Quantification of proliferating neointimal cells

Serial cross sections (5 μm thickness) of carotid arteries were made. One section was used for HE-staining to calculate the total cell number in the neointimal area, and the next section was used for PCNA immunohistochemistry. The total PCNA-immunopositive neointimal cells and total neointimal cells in HE-staining in each serial section were counted. Then, the percentage of PCNA-immunopositive cells per total number of neointimal cells in each section was calculated, and the average of the six sections per animal was obtained for each animal.

2.7. Detection of apoptosis in the neointimal cells

Apoptosis in the neointimal cells was detected by TUNEL technique. Modified TUNEL assay was performed by use of DeadEnd colorimetric apoptosis detection system (Promega) according to the manufacturer's instructions. Briefly, tissue sections from the neointima of PBS injected non-immunized group and rat VSMC-immunized group were washed in PBS, and endogenous peroxidase was blocked by 0.3% hydrogen peroxide. Biotinylated nucleotide was incorporated at the 3′-OH DNA ends using terminal deoxynucleotidyl transferase (TdT). Streptavidin-HRP was then bound to these biotinylated nucleotides, which were detected using hydrogen peroxide and diaminobenzidine (DAB). Some of slides were treated with Dnase I for positive controls. Stained cells were counted under a light microscope.

2.8. Immunoglobulin purification from rabbit plasma

The immunoglobulin from the pooled plasma derived from the rabbits on day 7 after the third immunization or from control rabbits was purified with the use of a Protein G column (Sigma, MO).

2.9. Immunoblotting using rabbit plasma and protein analysis

Rabbit VSMCs were primarily cultured by the explant method and cultured in DMEM with 10% fetal bovine serum (FBS). Rabbit VSMCs were homogenized in a homogenizing buffer containing 50 mM Tris–HCl (pH 7.4), 1 mM EDTA, 1 mM phenylmethyosulfonylfluoride, 10% glycerol, and 20 mM CHAPS. The whole protein (50 μg per lane) was resolved by SDS-PAGE (10% polyacrylamide), transferred to a PVDF membrane and probed with rabbit plasma obtained from PBS injected non-immunized control rabbits, rat hepatocyte-immunized control rabbits, or rat VSMC-immunized rabbits. Immunoreactive bands were visualized with horseradish peroxidase-conjugated anti-rabbit IgG (Amersham, England; 1:3000 dilution) and an ECL detection kit (Amersham, England).

2.10. Counting of VSMC number in vitro

Cell proliferation was quantified by total cell number as previously described [27]. Rabbit VSMCs (5000 per well) were seeded in 96-well microtiter plates in 0.1 mL of DMEM–10% FBS. After 12 h incubation, the medium was replaced by DMEM with purified immunoglobulin from rat hepatocyte-immunized group and that from rat VSMC-immunized group (20 μg/mL, respectively). At 48 h after stimulation with agonists (10% FBS, 1 μM ATII, 10 ng/ml PDGF-BB, 10 ng/ml FGF, 1 μM PMA), cells were fixed by addition of 10 μL of glutaraldehyde and shaken for 15 min. After being washed 3 times with deionized water, plates were air-dried and stained for 20 min with 0.1% crystal violet solution in 200 mM MES, pH 6.0. After being washed 3 times with deionized water to remove excess dye, plates were air-dried before solubilization of the bound dye in 10% acetic acid. The optical density of dye extracts was measured at 595 nm by using a microplate reader (Bio-Rad). Values are means±SEM of 8 separate experiments in each group.

2.11. VSMC migration

Rabbit VSMCs were grown to confluence in 6-well culture plates. The monolayer-wounding cell migration assay was performed as described previously [28,29]. Cell layers were scraped with a sterile single edged razor blade and re-incubated in DMEM containing 5 mM hydroxyurea with purified immunoglobulin from rat hepatocyte-immunized rabbits or rat VSMC-immunized rabbits (20 μg/mL, respectively). Hydroxyurea was added to eliminate any confounding effects of cell proliferation. At 24 h after stimulation with agonists (10% FBS, 1 μM ATII, 10 ng/ml PDGF-BB, 10 ng/ml FGF, 1 μM PMA), cells were fixed and the maximum migration distance across the wound edge was analyzed.

2.12. VSMC viability assay

Rabbit VSMCs (5000 per well) were incubated in 96-well plastic plates with purified immunoglobulin from rat VSMC-immunized rabbits or rat hepatocyte-immunized rabbits (20 μg/mL, respectively). After 24 h, cell viability was assessed by measuring mitochondrial NADH-dependent dehydrogenase activity with a Cell Counting Kit (Dojindo Molecular Technologies, Inc., Kumamoto, Japan) using sulfonated tetrazolium salt, 2-(4-iodophenyl)-3-(4-nitrophenyl)-5-(2,4-disulfophenyl)-2H-tetrazolium monosodium salt (WST-1) [30]. Each measurement was done in triplicate and the results

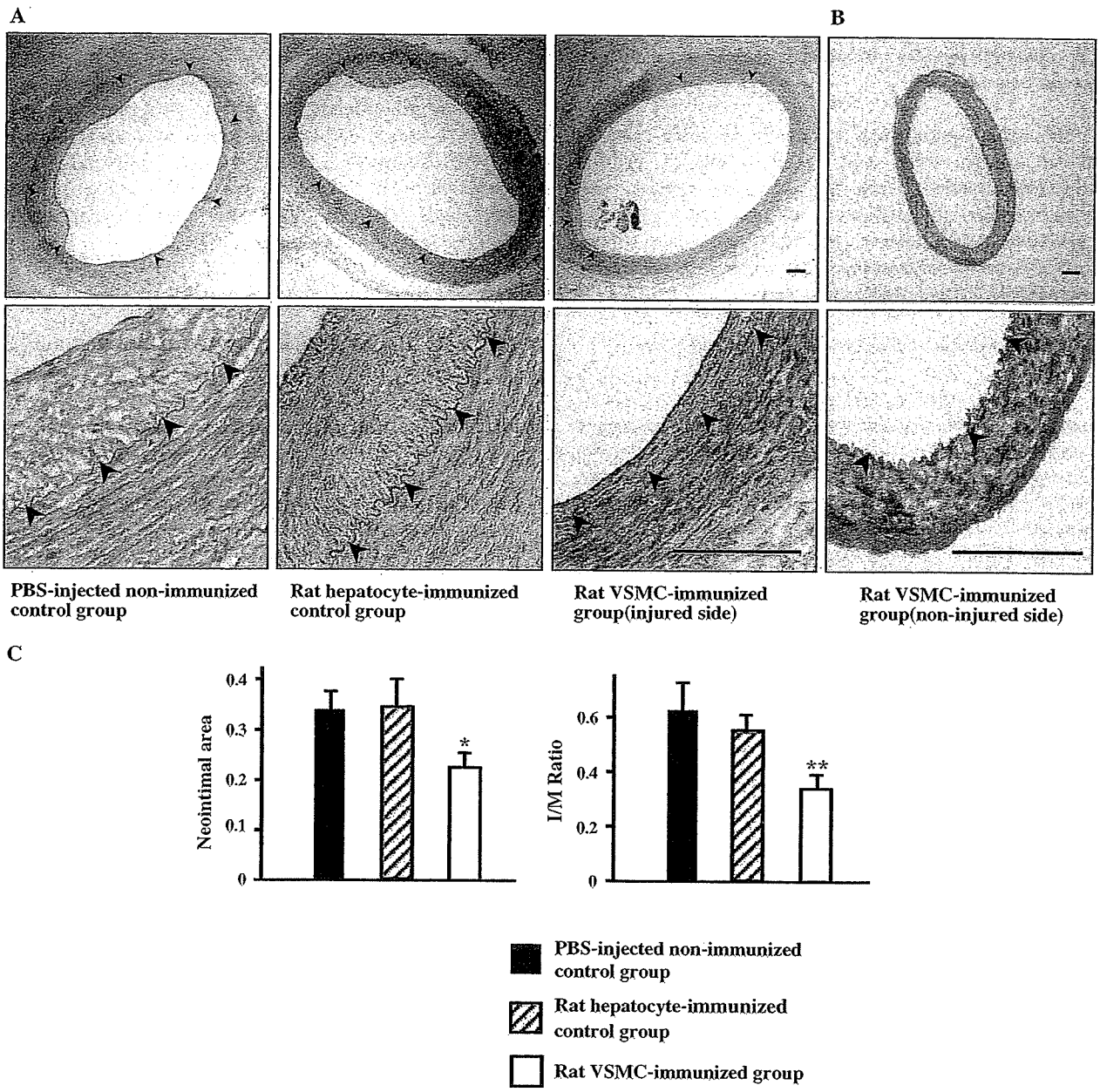

Fig. 1. (A) Representative light photomicrograph images showing injured carotid arteries from PBS-injected non-immunized control group, rat hepatocyte-immunized control group, and rat VSMC-immunized group at 4 weeks after balloon injury. Arrowhead indicates internal elastic lamina (IEL). Original magnifications are ×40 (upper) and ×200 (lower panels). Bars indicate 100 μm. (B) Representative light photomicrograph images showing the untouched contralateral common carotid artery from rat VSMC-immunized group. Arrowhead indicates internal elastic lamina (IEL). Original magnifications are ×40 (upper) and ×200 (lower panels). Bars indicate 100 μm. (C) Quantitative analysis of neointimal area and I/M ratio in rabbit carotid arteries at 4 weeks after injury in rat VSMC-immunized group (white bars), PBS-injected non-immunized control group (black bars), and rat hepatocyte-immunized control group (striped bars). Values are means ± SEM in each group. *$P<0.05$ vs. PBS-injected non-immunized control group and rat hepatocyte-immunized control group. **$P<0.05$ vs. PBS-injected non-immunized control group.

were presented as a percentage of the value for rat hepatocyte-immunized and control-immunized groups.

2.13. Identification of a target protein which rat VSMC-immunized immunoglobulin recognizes

Rabbit AT1a receptor cDNA was a generous gift from Dr. Raymond C. Harris (Vanderbilt Medical Center, Vanderbilt University). The complete coding site was excited and cloned into the expression vector pcDNA3 (Invitrogen), and pcDNA3 without any expression insert was used as the control vector. COS7 cells were purchased from the American Type Culture Collection (Manassas, VA) and cultured according to the manufacture's recommendations. COS7 cells were transfected by control pcDNA3 and rabbit AT1a receptor pcDNA3, respectively. The whole protein of these two groups of COS7 cells were resolved by SDS-PAGE, transferred to a PVDF membrane and probed with rabbit plasma obtained from PBS injected non-immunized control rabbits or rat hepatocyte-immunized control rabbits or rat VSMC-immunized rabbits respectively. Immunoreactive bands were visualized with horseradish peroxidase-conjugated anti-rabbit IgG (Amersham, England; 1:3000 dilution) and an ECL detection kit (Amersham, England).

2.14. Statistical analysis

Values represent means±SEM. Differences between groups were compared using a one-way analysis of variance test followed by Fisher protected least significant difference. $P<0.05$ was accepted as statistically significant.

3. Results

3.1. Blood analysis and general appearance of rabbits

Rat VSMC-immunization induced no significant changes in liver function, renal function and lipid profiles. Mean body weight and behavior of rabbits did not change by the immunization. In comparison with the PBS injected non-immunized control group, rat VSMC-immunization did not affect plasma IgG levels (284±61 mg/dl in PBS injected group vs. 268±44 mg/dl in rat VSMC-immunized group; P=NS).

3.2. Effect of rat VSMC immunization on the neointimal lesion formation

All animals developed concentric intimal lesions in response to the balloon injury. At 4 weeks after balloon injury, the mean neointimal area of PBS injected non-immunized group and rat hepatocyte-immunized control group were 0.339±0.036 and 0.350±0.041 mm^2, respectively (P=NS). The intimal lesion area was not significantly reduced by the rat hepatocytes control immunization. However, immunization with rat VSMCs significantly reduced the intimal lesion area (0.219±0.0286 mm^2; $P<0.05$ vs. PBS injected non-immunized group and rat

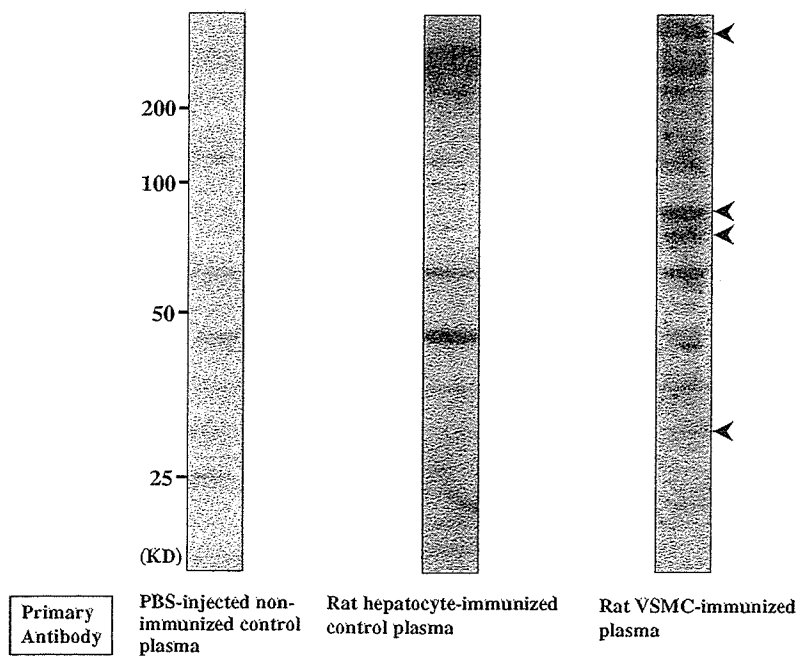

Fig. 2. Immunoblottings of proteins extracted from rabbit VSMCs using the plasma obtained from PBS injected non-immunized control rabbits (left), rat hepatocyte-immunized control rabbits (middle), or rat VSMC-immunized rabbits (right) as primary antibodies, respectively.

hepatocyte-immunized control group, Fig. 1A and C). The intimal/medial ratio was also significantly reduced in rat VSMC-immunized group (0.349±0.049) compared with PBS injected non-immunized group (0.662±0.114; $P<0.01$). There was no sign of infiltration of inflammatory cells at the contralateral common carotid artery (Fig. 1B). Immunization with rat VSMCs did not induce any pro-inflammatory effects on normal contractile VSMCs.

3.3. Rat VSMC immunization induced rabbit VSMC-reactive antibodies

To detect the antibodies, which were induced by xenogenic rat VSMC immunization, rabbit VSMCs proteins were resolved by SDS-PAGE, and immunoblotted with plasma obtained from the PBS injected non-immunized control rabbits, rat hepatocyte-immunized control rabbits ,

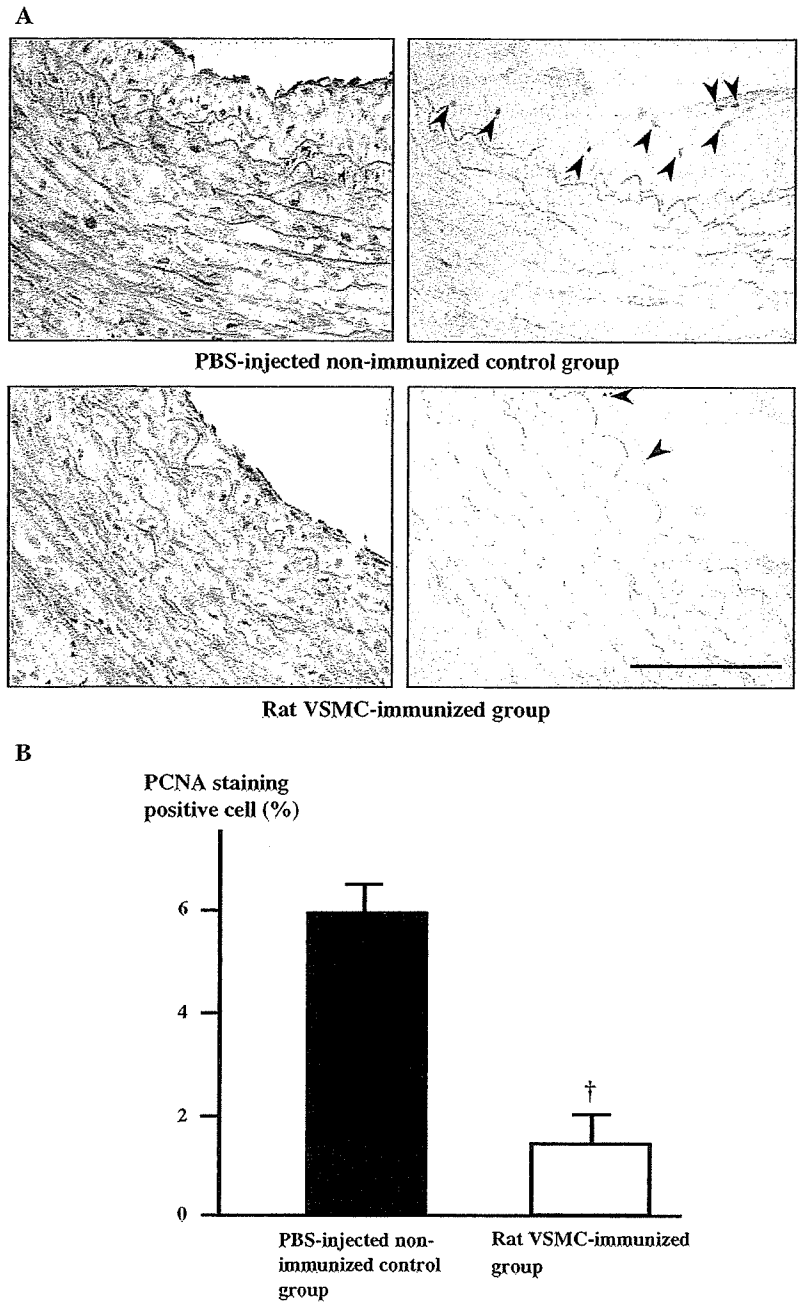

Fig. 3. (A) Photomicrographs of HE stainings (left panels) and PCNA immunostainings (right panels) in the neointima of injured carotid arteries at 2 weeks after balloon injury. Original magnification is ×200. A bar indicates 100 μm. (B) Quantitative analysis of PCNA positive proliferating cells in the neointima at 2 weeks after injury. Values are means±SEM of at least six rabbits in each group. †$P<0.01$ vs. PBS injected non-immunized control group.

or the VSMC-immunized rabbits. Only a few non-specific bands were detected when the plasma from the PBS injected non-immunized control rabbits was applied. Some bands were detected when the plasma from rat hepatocyte-immunized control rabbits was applied. In contrast, several new bands were clearly recognized in the immunoblot when we applied the plasma from rat VSMC-immunized rabbits (Fig. 2). It implies that the rat VSMC-immunized immunoglobulin recognized some new proteins of rabbit VSMCs that reacted with neither immunoglobulin from PBS injected non-immunized rabbits nor that from rat hepatocyte-immunized rabbits.

3.4. Effect of rat VSMC immunization on the proliferation and apoptosis of neointimal cells

To investigate whether the reduced neointimal lesion formation was due to the reduced proliferation of VSMCs in the neointimal lesion, the proliferation of neointimal VSMCs was investigated by the PCNA immunostaining on the day 14 after the injury (Fig. 3A). The percentage of PCNA-immunopositive cells was significantly reduced in VSMC-immunized group compared with in PBS injected control group (1.34%±0.49 vs. 5.78%±0.47, $P<0.01$, Fig. 3B).

Then to clarify the role of apoptosis in the reduction of neointimal formation, the TUNEL assay was carried out. As shown in Fig. 4, rat VSMC-immunization did not increase the number of TUNEL positive neointimal cells.

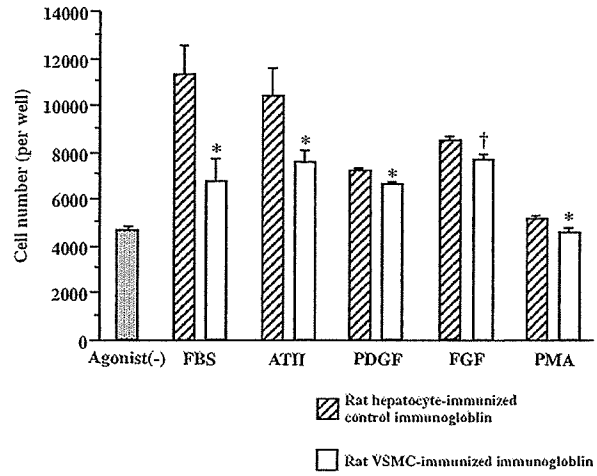

Fig. 5. Quantitative analysis of proliferation of cultured rabbit VSMCs treated with immunoglobulin obtained from rat hepatocyte-immunized control rabbits (striped bars) or rat VSMC-immunized rabbits (white bars). Values are means±SEM of separate six experiments in each group. †$P<0.01$ vs. the rat hepatocyte-immunized control group. *$P<0.05$ vs. PBS-injected non-immunized control group.

3.5. Effect of VSMC immunized immunoglobulins on rabbit VSMC proliferation and migration in vitro

The immunoglobulin (20 μg/ml) obtained from VSMC-immunized rabbits significantly suppressed rabbit VSMC cell numbers stimulated by FBS, ATII, PDGF, FGF, and PMA (Fig. 5) and rabbit VSMC migration stimulated by

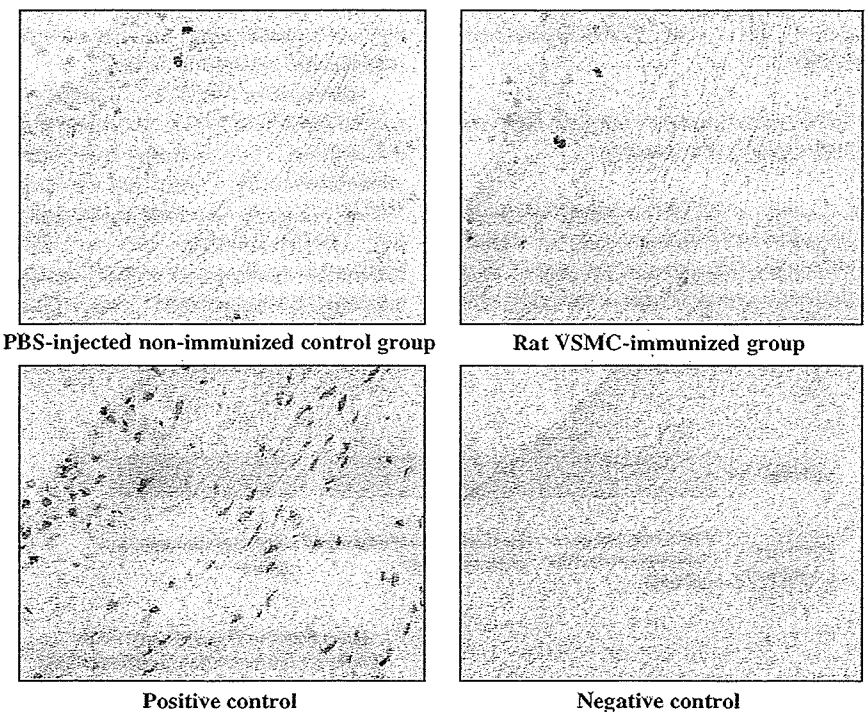

Fig. 4. Representative light photomicrograph images showing apoptosis in the neointimal cells using TUNEL technique.

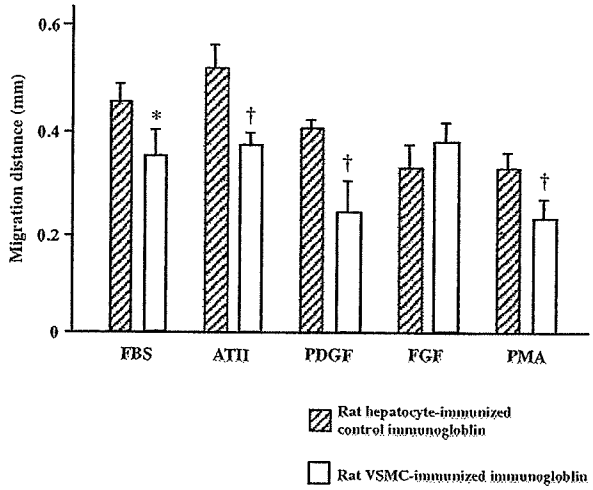

Fig. 6. Quantitative analysis of the migration distance evaluated by the maximally migrated point from the wounded edge in rat hepatocyte-immunized control group (striped bars) and in rat VSMC-immunized group (white bars), respectively. Values are means±SEM of five separate experiments in each group. †$P<0.01$ vs. the rat hepatocyte-immunized control group. *$P<0.05$ vs. PBS-injected non-immunized control group.

FBS, ATII, PDGF, and PMA (Fig. 6), compared with that from rat hepatocyte-immunized control rabbits.

3.6. Effect of immunized immunoglobulin on VSMC viability

The rat VSMC-immunized immunoglobulin used in the proliferation and the migration assays did not alter rabbit VSMC viability assessed by WST-1 assay (rat hepartocyte-immunized control group: 100% vs. rat VSMC-immunized group: 106±8.6%, P=NS).

3.7. AT1a receptor may be one of a target protein which rat VSMC-immunized immunoglobulin recognizes

As shown in Fig. 7, only rat VSMC-immunized rabbit plasma recognized the rabbit AT1a receptor protein which was expressed in COS7 cells by transfection of rabbit AT1a receptor pcDNA3 (molecular weight is about 50 kDa). No bands were detected by immunoglobulin from PBS-injected rabbits or that from hepatocyte-immunized rabbits.

4. Discussion

In the present study, we demonstrated for the first time that, immunization with xenogenic rat synthetic VSMCs reduced neointimal formation after balloon injury, in association with induction of auto-antibodies against rabbit VSMCs. The VSMCs which contribute to form neointimal lesions are different in phenotype from ones in the normal media [31]. VSMCs in the normal media consisted of a contractile phenotype, whereas VSMCs which contribute to form neointimal lesions show a synthetic phenotype [32]. And the epitopes of VSMCs also may be different between the contractile phenotype and the synthetic phenotype. We used cultured rat VSMCs as the xenogenic immunogens against rabbits. These rat VSMCs are the synthetic phenotype, and therefore immunization with rat VSMCs was likely to induce various antibodies against the synthetic VSMCs. And importantly, it seemed that certain antibodies cross-reacted between rat and rabbit VSMCs.

As demonstrated in Fig. 2, when we applied rat VSMC-immunized plasma as the primary antibody, several new proteins of rabbit VSMCs were detected by the Western blot analysis, which were not detected when PBS injected non-immunized control plasma or rat hepatocyte-immunized control plasma was applied It implies that the rabbit plasma obtained from rat VSMC-immunized rabbits had an antibody response distinct from the one induced by PBS or rat hepatocytes. Importantly, as demonstrated in Fig. 1, only rat VSMC-immunization reduced the neointimal lesion formation after balloon injury. These results might implicate that the induced antibodies reacting with the synthetic VSMCs but not others might play critical roles in the reduction of neointimal area in this study.

Apoptosis of VSMCs is implicated in the formation of neointimal lesions [33]. In the aortic allograft model in rats, Plissonnier et al. reported the induction of apoptosis by alloantisera [34]. Therefore, we investigated apoptosis of VSMCs in both the neointimal lesion and the normal media by TUNEL staining, but we did not find significant differences between rat VSMC-immunized group and PBS injected non-immunized group. On the other hand, the proliferative capability of VSMCs estimated by PCNA staining in neointimal lesions was significantly suppressed

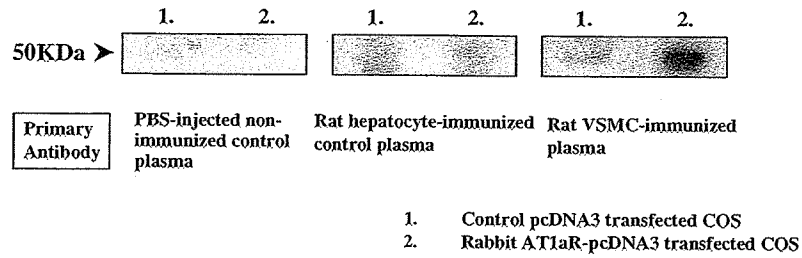

Fig. 7. The rabbit AT1a receptor protein expressed in COS7 cells by transfection of the rabbit AT1a receptor pcDNA3 was immunoblotted with PBS injected non-immunized control rabbit plasma (left panel), rat hapatocyte-immunized rabbit plasma (middle panel), or rat VSMC-immunized rabbit plasma (right panel), respectively. pcDNA3 without any expression inserts was used as the control transfection.

by rat VSMC-immunization (Fig. 3A and B), whereas no differences were detected in the media, at 2 weeks after balloon injury. Thus, proliferation of VSMCs in the neointima was suppressed by rat VSMC-immunization. This may be related to that neointimal lesions themselves may be more antigenic than the normal media. Plissonnier et al. reported that normal media was a "privileged" immunological site as compared to neointimal lesions in the vascular chronic rejection process in allotransplantation/immunization [35].

To further clarify the effects of the immunization on VSMC function, we performed in vitro assay. For in vitro assay, we purified immunoglobulin from plasma using a protein G column, because we needed to avoid the effects of many cytokines and growth factors which were contained in the immunized plasma. Therefore, in the study in vitro, we could investigate the direct effect of induced immunoglobulins. At first we compared viability of rabbit VSMCs between rat hepatocyte-immunized immunoglobulin treated control group and rat VSMC-immunized immunoglobulin treated group by use of WST-1 assay, and confirmed that viability of VSMC did not differ between two groups. Therefore VSMC-immunized immunoglobulin didn't have severe cell toxicity against VSMCs. The VSMC-immunized rabbits immunoglobulin significantly suppressed rabbit VSMC cell numbers stimulated by FBS, ATII, PDGF, FGF, and PMA (Fig. 5) and rabbit VSMC migration stimulated by FBS, ATII, PDGF, and PMA (Fig. 6). We applied immunoglobulins to the culture media, which bind only to the cell surface proteins. Therefore we speculate that rat VSMC-immunized immunoglobulin might bind to some surface proteins which globally regulate the proliferation and migration of rabbit VSMCs. As one of candidates for such surface proteins, we focused on AT1a receptor, since the inhibitory effects of VSMC-immunized rabbits immunoglobulin were prominent in ATII-induced proliferation and migration. As shown in Fig. 7, rat VSMC-immunized immunoglobulin was immunoreactive against the AT1a receptor protein which was expressed in COS7 cells by the rabbit AT1a receptor pcDNA3 transfection, whereas no bands were detected by immunoglobulin from PBS-injected rabbits or that from hepatocyte-immunized rabbits. Therefore, it is possible that rabbit AT1a receptor protein is one of target proteins which rat VSMC-immunized immunoglobulin recognizes and that binding of rat VSMC-immunized immunoglobulin to rabbit AT1a receptors might have inhibited the ATII signaling. Not only ATII signaling but almost all stimuli tested, however, were affected by the adjunction of rat VSMC-immunized immunoglobulin. Therefore it is likely that a much more global effect than the blocking effect on these receptors was involved. At the present time, we cannot show more detailed molecular mechanisms of the inhibitory effects of xenogenic VSMC immunization, and further investigation is needed.

This study demonstrated for the first time that xenogenic VSMC immunization significantly reduced neointimal formation in the balloon-injured carotid arteries. Our data indicate the possibility of immunotherapy for neointimal formation with xenogenic VSMCs by breaking immune tolerance against autologous VSMCs in a cross-reaction between the xenogenic homologs and self molecules, similar to the case of immunotherapy for tumor angiogenesis [36].

In the present study, rat VSMC-immunization didn't cause any serious side effects. The body weight and behavior of rabbits did not change by the immunization, and also blood analysis didn't show any significant changes in liver functions, renal functions, and lipid profiles. However, at the present time we cannot show the target protein(s) of VSMC-immunized immunoglobulin that regulates the functions of rabbit VSMC globally. Although further investigation on the target protein(s) and the possibility of immunological regulation is needed, immunological regulation shown in our study may be a new immunotherapy for vascular remodeling which forms neointimal lesion.

Acknowledgment

We appreciate Kiyoko Matsui for her secretarial assistance and technical support (cell culture, blood cell count, and animal care).

References

[1] Sriram V, Patterson C. Cell cycle in vasculoproliferative diseases: potential interventions and routes of delivery. Circulation 2001;103: 2414–9.
[2] Breuss JM, Cejna M, Bergmeister H, Kadl A, Baumgartl G, Steurer S, et al. Activation of nuclear factor-kappa B significantly contributes to lumen loss in a rabbit iliac artery balloon angioplasty model. Circulation 2002;105:633–8.
[3] Stabile E, Zhou YF, Saji M, Castagna M, Shou M, Kinnaird TD, et al. Akt controls vascular smooth muscle cell proliferation in vitro and in vivo by delaying G1/S exit. Circ Res 2003;93:1059–65.
[4] Zhan Y, Kim S, Izumi Y, Izumiya Y, Nakao T, Miyazaki H, et al. Role of JNK, p38, and ERK in platelet-derived growth factor-induced vascular proliferation, migration, and gene expression. Arterioscler Thromb Vasc Biol 2003;23:795–801.
[5] Palinski W, Miller E, Witztum JL. Immunization of low density lipoprotein (LDL) receptor-deficient rabbits with homologous malondialdehyde-modified LDL reduces atherogenesis. Proc Natl Acad Sci U S A 1995;92:821–5.
[6] Zhou X, Paulsson G, Stemme S, Hansson GK. Hypercholesterolemia is associated with a T helper (Th) 1/Th2 switch of the autoimmune response in atherosclerotic apo E-knockout mice. J Clin Invest 1998;101:1717–25.
[7] Mallat Z, Besnard S, Duriez M, Deleuze V, Emmanuel F, Bureau MF, et al. Protective role of interleukin-10 in atherosclerosis. Circ Res 1999;85:e17–24.
[8] Afek A, George J, Gilburd B, Rauova L, Goldberg I, Kopolovic J, et al. Immunization of low-density lipoprotein receptor deficient (LDL-RD) mice with heat shock protein 65 (HSP-65) promotes early atherosclerosis. J Autoimmun 2000;14:115–21.

[9] Rittershaus CW, Miller DP, Thomas LJ, Picard MD, Honan CM, Emmett CD, et al. Vaccine-induced antibodies inhibit CETP activity in vivo and reduce aortic lesions in a rabbit model of atherosclerosis. Arterioscler Thromb Vasc Biol 2000;20:2106–12.
[10] Zhou X, Nicoletti A, Elhage R, Hansson GK. Transfer of CD4(+) T cells aggravates atherosclerosis in immunodeficient apolipoprotein E knockout mice. Circulation 2000;102:2919–22.
[11] Zhou X, Caligiuri G, Hamsten A, Lefvert AK, Hansson GK. LDL immunization induces T-cell-dependent antibody formation and protection against atherosclerosis. Arterioscler Thromb Vasc Biol 2001;21:108–14.
[12] Caligiuri G, Nicoletti A, Poirier B, Hansson GK. Protective immunity against atherosclerosis carried by B cells of hypercholesterolemic mice. J Clin Invest 2002;109:745–53.
[13] Maron R, Sukhova G, Faria AM, Hoffmann E, Mach F, Libby P, et al. Mucosal administration of heat shock protein-65 decreases atherosclerosis and inflammation in aortic arch of low-density lipoprotein receptor-deficient mice. Circulation 2002;106:1708–15.
[14] Binder CJ, Horkko S, Dewan A, Chang MK, Kieu EP, Goodyear CS, et al. Pneumococcal vaccination decreases atherosclerotic lesion formation: molecular mimicry between *Streptococcus pneumoniae* and oxidized LDL. Nat Med 2003;9:736–43.
[15] Caligiuri G, Rudling M, Ollivier V, Jacob MP, Michel JB, Hansson GK, et al. Interleukin-10 deficiency increases atherosclerosis, thrombosis, and low-density lipoproteins in apolipoprotein E knockout mice. Mol Med 2003;9:10–7.
[16] Fredrikson GN, Hedblad B, Berglund G, Alm R, Ares M, Cercek B, et al. Identification of immune responses against aldehyde-modified peptide sequences in apoB associated with cardiovascular disease. Arterioscler Thromb Vasc Biol 2003;23:872–8.
[17] Fredrikson GN, Soderberg I, Lindholm M, Dimayuga P, Chyu KY, Shah PK, et al. Inhibition of atherosclerosis in apoE-null mice by immunization with apoB-100 peptide sequences. Arterioscler Thromb Vasc Biol 2003;23:879–84.
[18] Mallat Z, Gojova A, Brun V, Esposito B, Fournier N, Cottrez F, et al. Induction of a regulatory T cell type 1 response reduces the development of atherosclerosis in apolipoprotein E-knockout mice. Circulation 2003;108:1232–7.
[19] Robertson AK, Rudling M, Zhou X, Gorelik L, Flavell RA, Hansson GK. Disruption of TGF-beta signaling in T cells accelerates atherosclerosis. J Clin Invest 2003;112:1342–50.
[20] Schiopu A, Bengtsson J, Soderberg I, Janciauskiene S, Lindgren S, Ares MP, et al. Recombinant human antibodies against aldehyde-modified apolipoprotein B-100 peptide sequences inhibit atherosclerosis. Circulation 2004;110:2047–52.
[21] Tupin E, Nicoletti A, Elhage R, Rudling M, Ljunggren HG, Hansson GK, et al. CD1d-dependent activation of NKT cells aggravates atherosclerosis. J Exp Med 2004;199:417–22.
[22] Nilsson J, Hansson GK, Shah PK. Immunomodulation of atherosclerosis: implications for vaccine development. Arterioscler Thromb Vasc Biol 2005;25:18–28.
[23] Nilsson J, Calara F, Regnstrom J, Hultgardh-Nilsson A, Ameli S, Cercek B, et al. Immunization with homologous oxidized low density lipoprotein reduces neointimal formation after balloon injury in hypercholesterolemic rabbits. J Am Coll Cardiol 1997;30:1886–91.
[24] Hayashi S, Watanabe N, Nakazawa K, Suzuki J, Tsushima K, Tamatani T, et al. Roles of P-selectin in inflammation, neointimal formation, and vascular remodeling in balloon-injured rat carotid arteries. Circulation 2000;102:1710–7.
[25] Hamaguchi A, Kim S, Izumi Y, Zhan Y, Yamanaka S, Iwao H. Contribution of extracellular signal-regulated kinase to angiotensin II-induced transforming growth factor-beta1 expression in vascular smooth muscle cells. Hypertension 1999;34:126–31.
[26] Faggin E, Puato M, Zardo L, Franch R, Millino C, Sarinella F, et al. Smooth muscle-specific SM22 protein is expressed in the adventitial cells of balloon-injured rabbit carotid artery. Arterioscler Thromb Vasc Biol 1999;19:1393–404.
[27] Kueng W, Silber E, Eppenberger U. Quantification of cells cultured on 96-well plates. Anal Biochem 1989;182:16–9.
[28] Sarkar R, Meinberg EG, Stanley JC, Gordon D, Webb RC. Nitric oxide reversibly inhibits the migration of cultured vascular smooth muscle cells. Circ Res 1996;78:225–30.
[29] Pukac L, Huangpu J, Kamovsky MJ. Platelet-derived growth factor-BB, insulin-like growth factor-I, and phorbol ester activate different signaling pathways for stimulation of vascular smooth muscle cell migration. Exp Cell Res 1998;242:548–60.
[30] Mosmann T. Rapid colorimetric assay for cellular growth and survival: application to proliferation and cytotoxicity assays. J Immunol Methods 1983;65:55–63.
[31] Nobuyoshi M, Kimura T, Ohishi H, Horiuchi H, Nosaka H, Hamasaki N, et al. Restenosis after percutaneous transluminal coronary angioplasty: pathologic observations in 20 patients. J Am Coll Cardiol 1991;17:433–9.
[32] Thyberg J, Blomgren K, Hedin U, Dryjski M. Phenotypic modulation of smooth muscle cells during the formation of neointimal thickenings in the rat carotid artery after balloon injury: an electron-microscopic and stereological study. Cell Tissue Res 1995;281:421–33.
[33] Mayr M, Xu Q. Smooth muscle cell apoptosis in arteriosclerosis. Exp Gerontol 2001;36:969–87.
[34] Plissonnier D, Henaff M, Poncet P, Paris E, Tron F, Thuillez C, et al. Involvement of antibody-dependent apoptosis in graft rejection. Transplantation 2000;69:2601–8.
[35] Plissonnier D, Nochy D, Poncet P, Mandet C, Hinglais N, Bariety J, et al. Sequential immunological targeting of chronic experimental arterial allograft. Transplantation 1995;60:414–24.
[36] Wei YQ, Wang QR, Zhao X, Yang L, Tian L, Lu Y, et al. Immunotherapy of tumors with xenogeneic endothelial cells as a vaccine. Nat Med 2000;6:1160–6.

Research Paper

Journal of Vascular Research

J Vasc Res 2006;43:131–138
DOI: 10.1159/000090132

Received: March 28, 2005
Accepted after revision: September 23, 2005
Published online: December 7, 2005

Endothelial Urocortin Has Potent Antioxidative Properties and Is Upregulated by Inflammatory Cytokines and Pitavastatin

Tomoyuki Honjo[a] Nobutaka Inoue[a] Rio Shiraki[a] Seiichi Kobayashi[a]
Kazunori Otsui[a] Motonori Takahashi[a] Ken-ichi Hirata[a]
Seinosuke Kawashima[a] Hiroshi Yokozaki[b] Mitsuhiro Yokoyama[a]

[a]Division of Cardiovascular and Respiratory Medicine, Department of Internal Medicine, and [b]Division of Surgical Pathology, Department of Biological Informatics, Kobe University Graduate School of Medicine, Kobe, Japan

Key Words
Endothelium · Oxidative stress · HMG-CoA reductase inhibitors

Abstract
Background: Urocortin, a neuropeptide discovered in the midbrain, is a member of the corticotropin-releasing factor family and is expressed in heart tissues. Urocortin exerts potent cardioprotective effects under various pathological conditions including ischemia/reperfusion. However, the regulation and function of vascular urocortin are unknown. ***Methods and Results:*** Immunohistochemistry showed definitive expression of urocortin in endothelial cells of coronary large arteries and microvessels from autopsied hearts. RT-PCR confirmed the expression of urocortin in human umbilical vein endothelial cells (HUVECs). Urocortin (10^{-8} *M*) potently suppressed the generation of angiotensin II-induced reactive oxygen species (ROS) in HUVECs. Tumor necrosis factor-α and interferon-γ increased the urocortin mRNA levels and its release from HUVECs. Incubation with pitavastatin (0.1–3.0 μ*M*) significantly increased the urocortin mRNA levels and its release from HUVECs. Furthermore, treatment with pitavastatin (2 mg/day) for 4 weeks increased the serum urocortin level from 11.0 ± 6.5 to 16.4 ± 7.3 ng/ml in healthy volunteers. ***Conclusion:*** Endothelial urocortin was upregulated by inflammatory cytokines and pitavastatin and suppressed ROS production in endothelial cells. Treatment with pitavastatin increased the serum urocortin level in human subjects. Thus, endothelial urocortin might protect cardiomyocytes in inflammatory lesions. Urocortin might partly explain the mechanisms of various pleiotropic effects of statins.

Introduction

Urocortin is a 40-amino-acid peptide originally discovered in the rat midbrain and a member of the corticotropin-releasing factor (CRF) family [1]. Human urocortin is expressed not only in the central nervous system, such as in the pituitary [2] and brain [3], but also in various peripheral tissues, including the placenta [4], gastrointestinal tract [5], synovial tissue [6], lymphocytes [7], adipose tissue [8] and heart [9]. These findings suggest that urocortin has some pathophysiologic roles in these peripheral tissues. Especially in the heart, exogenous administration of urocortin induces cardiac inotropic ef-

KARGER
Fax +41 61 306 12 34
E-Mail karger@karger.ch
www.karger.com

1018–1172/06/0432–0131$23.50/0

Accessible online at:
www.karger.com/jvr

Dr. Nobutaka Inoue
Division of Cardiovascular and Respiratory Medicine, Department of Internal Medicine
Kobe University Graduate School of Medicine
7-5-2 Kusunoki-cho, Chuo-ku, Kobe 650-0017 (Japan)
Tel. +81 78 382 5846, Fax +81 78 382 5859, E-Mail nobutaka@ri.nevc.go.jp

fects and coronary vasodilation [10–12]. Moreover, it was reported that exogenous urocortin has potent protective effects on myocardial cells during ischemia. For example, urocortin increases the survival of cultured cardiac cells exposed to ischemia and also rescues the infarct area of rat heart during ischemia/reperfusion [13–17].

The actions of the CRF family peptides are mediated by at least two types of G-protein-coupled receptors, CRF-R1 and CRF-R2 [1]. CRF-R2 exists in three alternative spliced forms, i.e., CRF-R2α, R2β, and R2γ. CRF-R2 is expressed in the cardiovascular system [18, 19], and has higher affinity for urocortin than CRF. Wiley et al. [19] reported that urocortin produced a potent and sustained vasodilator response in isolated human internal mammary artery. The coexpression of CRF-R2 with its preferred urocortin ligand in the heart suggests that urocortin-induced cardioprotective effects are likely mediated by CRF-R2 in an autocrine/paracrine manner [20]. Recently, Florio et al. [21] reported that urocortin is expressed in vessel walls. Furthermore, previous investigations demonstrated that CRF-R2 exists in cultured human umbilical vein endothelial cells (HUVECs) [22]. However, the vascular action of urocortin and its regulation remain unknown.

On the other hand, there is accumulating evidence that besides its potent lipid-lowering effect, HMG-CoA reductase inhibitors have pleiotropic effects such as anti-inflammatory [25, 26], anti-proliferative and anti-oxidative effects [27]. These drugs improve endothelial dysfunction in various pathologic conditions and stabilize vulnerable plaques via suppression of inflammation [28]. More recently, Node et al. [23] reported that HMG-CoA reductase inhibitors improve cardiac function in patients with heart failure. The potent cardioprotective effects suggest that the pleiotropic effects of HMG-CoA reductase inhibitors are related to urocortin.

In the present study, we investigated whether urocortin is expressed in human endothelial cells. We also investigated the vascular action of urocortin and what factors regulate the expression of endothelial urocortin. Furthermore, the interaction of urocortin and HMG-CoA reductase inhibitor was investigated.

Methods

Cell Culture

HUVECs were obtained from Sanko Junyaku (Japan) and cultured in Medium 199 with 20% fetal bovine serum (FBS), 100 IU/ml heparin (Sigma Chemical Co., St. Louis, Mo., USA), 100 IU/ml endothelial cell growth supplement (BD Biosciences, Franklin Lakes, N.J., USA), 100 U/ml penicillin, and 100 μg/ml streptomycin. Cells were used between passages 4 and 8. Cells were stimulated with tumor necrosis factor-α (TNF-α), interferon-γ (IFN-γ), or pitavastatin at various concentrations for the indicated hours (0, 3, 6, and 24 h) in the presence of 5% FBS. Human recombinant TNF-α and IFN-γ were purchased from R&D Systems, Inc. (Mckinley Place NE, Minn., USA) and Diaclone Research (France), respectively. Pitavastatin was obtained from Kowa Pharmaceutical Company (Tokyo, Japan). After stimulation, the culture medium was collected for enzyme-linked immunosorbent assay (ELISA), and the cells were used for RNA isolation.

Measurement of Urocortin by ELISA

Serum urocortin and supernatants of cell culture medium were assayed by ELISA (Phoenix Pharmaceuticals Inc., Belmont, Calif., USA) according to the manufacturer's instructions. Assays were performed in polystyrene 96-well plates. The urocortin concentration was quantified against a standard curve calibrated with known amounts of protein. The upper detection limit for urocortin was 100 ng/ml. Each value is the mean of duplicate measurements.

Human Blood Sample and Study Design

Fifteen male volunteers, 25–41 years old, were included in the study. Participants were examined to exclude any pathologic disorders, which was confirmed with blood tests. Three volunteers were excluded because of mildly elevated levels of creatine phosphokinase or C-reactive protein (CRP). The remaining healthy subjects were treated with pitavastatin (2 mg/day) for 4 weeks. Blood samples were collected before and after pitavastatin treatment, and serum levels of lipids, CRP, and urocortin were measured. There were no reported adverse effects of pitavastatin. Written informed consent was obtained from all participants.

Immunohistochemistry

Immunohistochemistry for urocortin was performed on serial cryostat sections cut at 6 μm from frozen human coronary artery and heart muscle specimens. The sections were blocked with carrier protein for 30 min at room temperature, and then incubated with a primary antibody (rabbit anti-urocortin, IgG fraction of antiserum, Sigma Chemical Co.) (diluted 1:200) overnight at 4°C. The final concentration of primary antibody was 40 μg/ml. The sections were washed with phosphate-buffered saline (PBS), incubated with biotinylated goat anti-rabbit immunoglobulins (Dako) (diluted 1:500), washed in PBS, and finally incubated with streptavidin horseradish peroxidase conjugate (Dako LSAB kit™, Dako). For negative controls, the primary antibody was replaced with rabbit nonspecific immunoglobulin.

Reverse Transcription PCR and Measurement of Urocortin RNA Level

Total RNA was isolated from cultured HUVECs using a total RNA isolation kit (Isogen; Nippon Gene, Japan) according to the manufacturer's instructions. Complementary DNA was prepared using an RT-PCR kit (RETROscript™; Ambion). PCR were performed with *Taq* polymerase using the following specific primers. The primer sequences were as follows: human urocortin sense primer 5′-CAGGCGAGCGGCCGCG-3′, human urocortin antisense primer 5′-CTTGCCCACCGAGTCGAAT-3′. Urocortin cDNA amplification was performed in 40 cycles: samples were heated to 94°C for 1 min, cooled to 60°C for 1 min, and then heat-

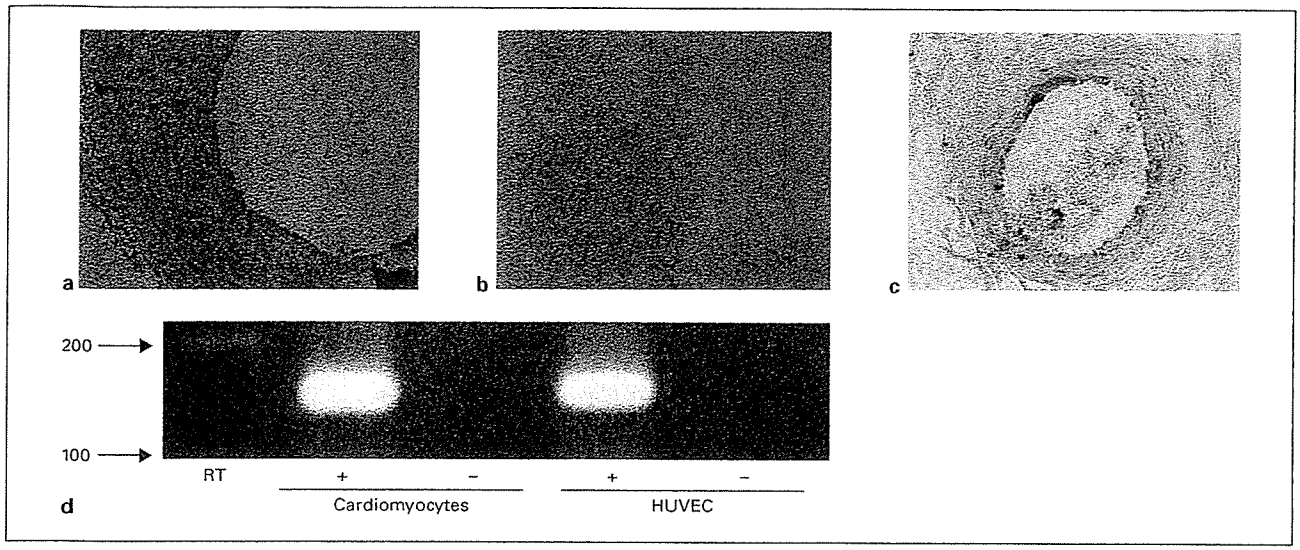

Fig. 1. Expression of urocortin in human endothelial cells. **a**, **c** Immunohistochemical analysis using epicardial coronary arteries (**a**) and microvessels in heart muscle (**c**) obtained from autopsy cases demonstrated positive urocortin immunoreactivity. **b** There was no significant staining when nonimmune serum was used as a control. **d** RT-PCR confirmed the expression of urocortin in cultured HUVECs. Human cardiomyocytes were used as a positive control.

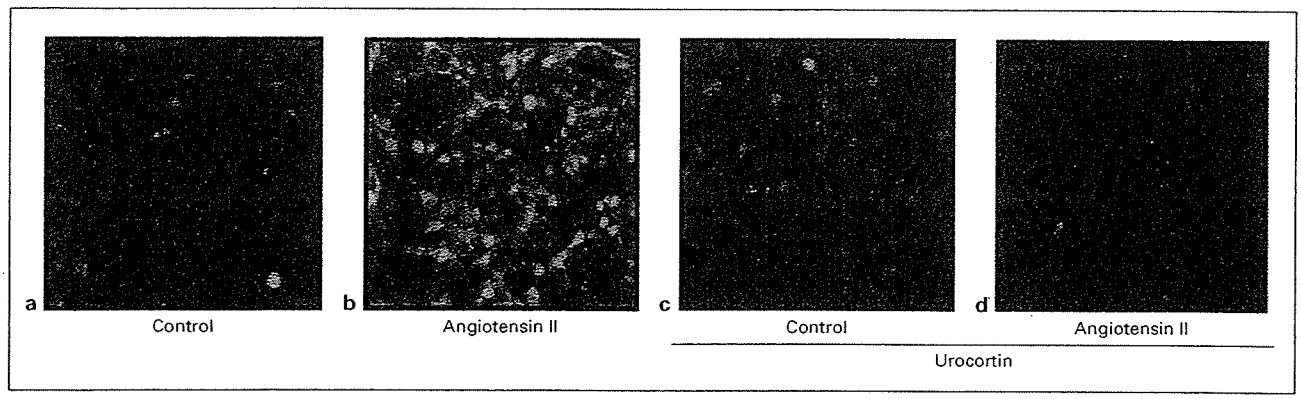

Fig. 2. Effects of urocortin on intracellular ROS in HUVECs assessed by the H_2DCFDA method. **a**, **b** Incubation with angiotensin II (10^{-7} *M*) induced the generation of intracellular ROS in HUVECs. **c**, **d** Coincubation with urocortin (10^{-8} *M*) significantly suppressed angiotensin II-induced intracellular ROS generation.

ed at 72°C for 1 min. PCR products were separated using 2% agarose gels stained with ethidium bromide and visualized under UV light. PCR products were purified and further analyzed by DNA sequencing using an ABI Prism BigDye Terminator Cycle Sequencing kit on an ABI Prism 310 Genetic Analyzer. To measure the production of urocortin mRNA, RT-PCR for GAPDH was also performed (sense primer 5′-ACGGATTTGGTCGTATTGGGC-3′, antisense primer 5′-TTGACGGTGCCATGGAATTTG-3′). Photographs of the ethidium-bromide-stained gels were scanned, and band intensities were measured using a densitometer (ATTO Lane Analyzer 3.0; ATTO Co., Tokyo, Japan). The quantity of the urocortin mRNA was determined by the ratio of urocortin and GAPDH band intensities.

Evaluation of Intracellular ROS in HUVECs

Intracellular ROS were detected with 2′,7-dichlorodihydrofluoresceindiacetate (H_2DCFDA, Molecular Probes, Eugene, Oreg., USA). As described before [31], a confluent monolayer of HUVECs was treated with angiotensin II (10^{-7} *M*) (Sigma Chemical Co.) or human urocortin (10^{-8} *M*) (Phoenix Pharmaceuticals Inc.) for 1 h,

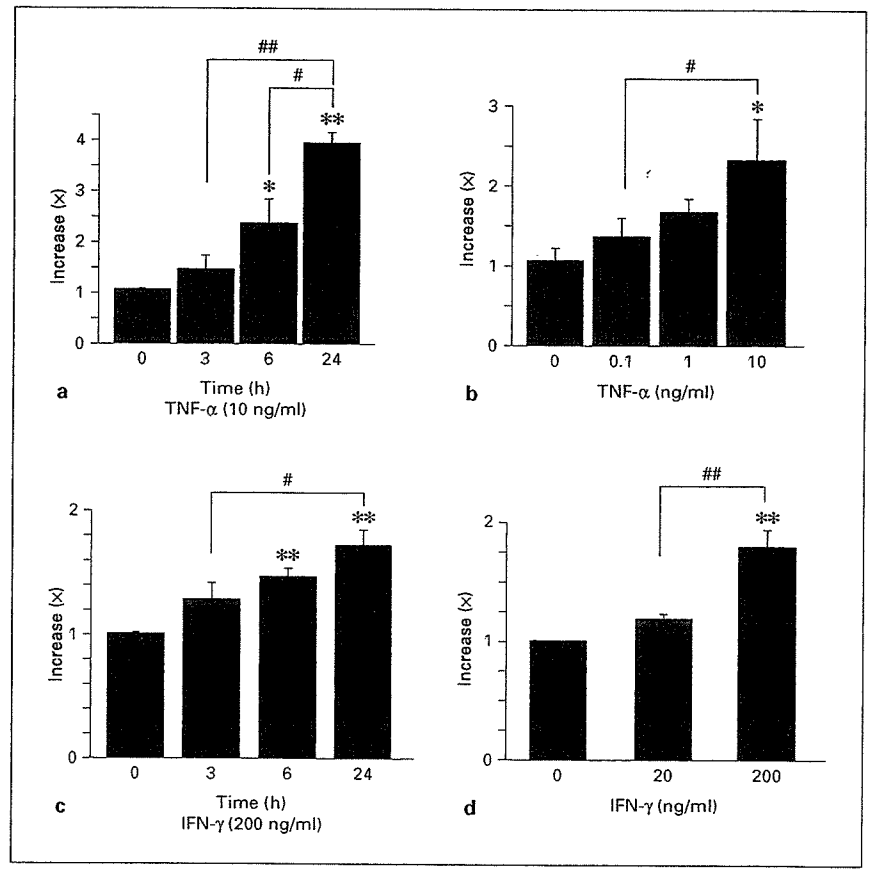

Fig. 3. Effects of TNF-α (**a**, **b**) or IFN-γ (**c**, **d**) on the release of urocortin from HUVECs. **a**, **b** HUVECs were incubated with TNF-α (10 ng/ml) for the indicated time periods (**a**) or for 6 h with the indicated concentration of TNF-α (**b**). **c**, **d** HUVECs were incubated with IFN-γ (200 ng/ml) for the indicated time periods (**c**) or for 6 h with the indicated concentration of IFN-γ (**d**). After stimulation, the concentration of urocortin in the conditioned medium was assessed by ELISA. Data were plotted as mean ± SEM from three independent experiments performed in duplicate. * $p < 0.05$; ** $p < 0.01$ vs. control; # $p < 0.05$; ## $p < 0.01$.

then they were treated with H_2DCFDA (10 μ*M*) for 30 min at 37°C in the dark. The fluorescence intensity was measured using a laser-scanning confocal imaging system.

Statistical Analysis

Data are presented as mean ± SEM. Statistical analysis was performed by analysis of variance followed by Fisher's PLSD test. $p < 0.05$ was considered to be statistically significant.

Results

Human Endothelial Cells Express Urocortin

First, we examined whether human endothelial cells express urocortin. As shown in figure 1, immunohistochemical analysis using specimens obtained from autopsy cases demonstrated positive immunoreactivity of urocortin in human epicardial coronary artery endothelial cells (fig. 1a) and endothelial cells of microvessels in heart muscle (fig. 1c), whereas there was no signal when non-immune serum was used (fig. 1b). Preabsorbance of the primary antibody with 10^{-8}–10^{-6} *M* of urocortin significantly suppressed the immunoreactivity. Next, to confirm its expression in endothelial cells, RT-PCR was performed using sets of urocortin-specific primers. Urocortin mRNA was detected by RT-PCR in HUVECs (fig. 1d). No RT-PCR product was present in the negative control in which RT was not performed. Sequencing of complementary DNA of urocortin obtained from HUVECs was the same as the sequence obtained from neurons (data not shown). Thus, urocortin is expressed in human endothelial cells.

Urocortin Suppressed ROS Generation in HUVECs

We investigated the effects of urocortin on ROS generation of HUVECs by H_2DCFDA. Incubation with angiotensin II (10^{-7} *M*) induced the generation of ROS in HUVECs (fig. 2). Urocortin (10^{-8} *M*) significantly suppressed angiotensin II-induced ROS generation.